DWR-1249

Estimation of Adult Delta Smelt Distribution for Hypothesized Swimming Behaviors Using Hydrodynamic, Suspended Sediment and Particle-Tracking Models

Prepared by:
Resource Management Associates
1840 San Miguel Dr., Suite 102
Walnut Creek, CA 94596
Contact: Edward Gross
925-300-3387

RMA Resource Management Associates

Prepared for

Collaborative Adaptive Management Team

US Fish and Wildlife Service

Investigators

Edward Gross (RMA)
Benjamin Saenz (RMA)
Richard Rachiele (RMA)
Stacie Grinbergs(RMA)
Lenny Grimaldo (ICF)
Josh Korman (Ecometric)
Pete Smith (USGS retired)
Michael MacWilliams (Anchor QEA)
Aaron Bever (Anchor QEA)

Executive Summary

This hydrodynamic and particle-tracking study was tasked by the Delta Smelt Scoping Team (DSST) of the Collaborative Adaptive Management Team (CAMT) as part of the Investigations on Understanding Population Effects and Factors that Affect Entrainment of Delta Smelt at State Water Project (SWP) and Central Valley Project (CVP) Export Facilities. Additional funding was provided by US Fish and Wildlife Service for preparation of this report which documents a portion of the CAMT study entitled Modeling Delta Smelt Movement into the South Delta: Linking Behavior, Habitat Suitability and Hydrodynamics to Better Understand Entrainment at the State Water Project and Central Valley Project. This report documents a subset of the CAMT work funded by USFWS, focusing on contrasting distribution resulting from hypothesized behaviors of adult delta smelt during their spawning migration.

This report documents particle-tracking model (PTM) results for different hypothesized swimming behavior rules. The hypothesized behaviors were developed after consultation with the Delta Smelt Scoping Team, the Independent Review Panel and other experts. This report is limited to simulations in which both the release time and release distribution of particles are specified a priori. In contrast, additional work documented in Korman et al. (2018) includes statistical fitting of initial distribution most consistent with observations including catch in Spring Kodiak Trawl. Because the PTM simulations for the next phase of work track particles released in 15 different regions through time they are computationally intensive relative to the simulations documented here which involve only a single release region, located on the lower Sacramento River.

Two periods were chosen for this evaluation of behavior rules. Water year 2002 was chosen as a year with a clear signal in salvage of delta smelt, and was simulated both with two-dimensional (2D) and three-dimensional (3D) modeling tools. Water year 2004 was chosen due to a double peak in observed salvage which is particularly challenging to reproduce with particle-tracking modeling. This report explores not only the relative performance of different behavior rules but also documents application of two independent sets of modeling tools, 2D and 3D, for 2002. The predicted distribution and entrainment during an additional water year (2004) is also estimated for each set of behavior rules using the 2D tools.

A set of 3D modeling tools have been applied in this study. The UnTRIM 3D hydrodynamic model (Casulli and Walters 2000) was applied with the SediMorph sediment transport model (BAW 2005) to predict water level, current speed, salinity, suspended sediment and turbidity in December 2010 and January 2011 and December 2001 through April 2002. The SWAN model (2009) was used to estimate wind wave period and height for use in bed shear stress estimates. The hydrodynamic calibration of this model is documented by MacWilliams et al (2015) and the sediment transport model is documented in Bever and MacWilliams (2013). The calibration for this project is documented in a CAMT report (Anchor QEA 2017). The hydrodynamic and turbidity predictions are used in a particle-tracking model (Ketefian et al. 2016) with an individual-based model of fish, involving swimming rules that describe delta smelt swimming responses to environmental stimuli. Broadly, the hypothesized swimming behavior rules represented possible delta smelt swimming responses to different environmental stimuli.

An independent set of 2D modeling tools were used to model depth-averaged hydrodynamics, salinity and suspended sediment, and particle tracking. Similar to a previous study concerning the spawning migration of Delta smelt (RMA 2009), the RMA2 finite element model (King, 1986) and associated tools simulated hydrodynamics and sediment transport and the RMA PTRK particle-tracking model was used

to represent delta smelt. The calibration of the hydrodynamic and sediment transport modeling tools is documented in a separate report to CAMT (RMA 2017).

For both the 3D and 2D particle-tracking models, a new swimming behavior module was developed as part of this project. The codes are distinct for each of the two particle tracking models, but they share a common input file and permit identical modeled swimming behavior in 2D and 3D. The sets of behavior rules that can be explored using these tools is described in detail.

The delta smelt distribution is predicted using different sets of behavior rules through each winter-spring simulation period, and evaluated using both qualitative and quantitative metrics. Qualitative metrics include retention in the Delta and quantitative metrics include consistency of the predicted delta smelt distribution with observed patterns of distribution in the Spring Kodiak Trawl data and the timing of salvage. In this report, we assume a fixed initial particle/fish distribution in order to better isolate differences between behaviors (all behaviors have the same initial distribution) and provide comparisons between observations and predicted distributions and entrainment.

Introduction

Delta smelt is an endangered fish species endemic to the upper San Francisco Estuary whose population has declined rapidly, particularly as part of the "pelagic organism decline" starting in the early 2000s (Thompson et al. 2010). Although several factors have been implicated in its decline, including a diminished food supply (Sommer et al. 2007), contaminants (Hammock et al. 2016) loss of habitat (Feyrer et al. 2007) and other changes to the environment (Moyle et al 2016), entrainment losses at the State Water Project (SWP) and Central Valley Project (CVP) garner significant attention because they are one factor that can be directly managed through water export reductions to minimize direct mortality to the Delta Smelt population. A greater understanding of factors that contribute to entrainment losses is desired to improve both management of the species and water export supplies (Brown et al. 2009).

One the greater sources of uncertainty in managing SWP and CVP exports to minimize entrainment impacts to delta smelt is understanding the mechanisms that attract them into the vicinity of the exports. From summer to fall, delta smelt are typically observed in turbid habitats in the low salinity zone (Feyrer et al. 2007) or in the northern freshwater region of the estuary (Cache Slough Complex; Sommer and Mejia 2013). Both these regions are situated outside substantial hydrodynamic influence of SWP and CVP exports and delta smelt are not salvaged at the SWP and CVP during these seasons. Prior to 1990, some delta smelt were found in the south Delta and were salvaged during summer and fall months. In recent decades, water clarity has substantially increased in the south Delta (Schoellhamer 2011), which may explain why delta smelt are no longer found in the south Delta from summer to fall. In contrast, during the winter, some proportion of the delta smelt population disperses into the vicinity of the SWP and CVP. These movements typically coincide with the onset of large precipitation events that transport suspended sediment (and associated turbidity) into the estuary (Grimaldo et al 2009). Also known as "first flush" periods, these events historically led to substantial salvage events within days of increased turbidity (Grimaldo et al. 2009). These salvage observations, along with targeted field studies of Delta Smelt during first flush periods (Bennett and Burau 2014), suggest that Delta Smelt behavior triggered by a change in available upstream habitat or their internal physiology (e.g., reproductive readiness) facilitates a rapid distribution shift to landward habitats not occupied during the summer and fall. Note, some delta smelt appear to remain in local tributaries and marsh habitats (Murphy and Hamilton 2013), and others appear to shift geographically seaward (i.e., to Napa River) depending on the amount of freshwater outflow.

The purpose of the study documented here and in Korman et al. (2018) is to evaluate hypothesized adult delta smelt swimming behaviors and understand how those behaviors, driven by the environmental conditions of turbidity, salinity, and Delta flows, may affect predicted adult delta smelt distribution and entrainment at the south Delta export facilities. We explore several types of behaviors guided by existing literature on delta smelt behavior, guidance from the Delta Smelt Scoping Team (DSST), and the Independent Review Panel (IRP) review of the CAMT proposal for delta smelt investigations. Our general conceptual model is that a landward migration of mature delta smelt in late fall or early winter is triggered by changes in turbidity distribution, or possibly salinity distribution. We hypothesize that delta smelt swimming may respond to the magnitude or spatial gradients of velocity, water depth, turbidity and salinity. While additional environmental cues, such as water temperature or food availability, may influence delta smelt movement, they are not explored in this work.

One hypothesized behavior is tidal migration ("tidal surfing"; Sommer et al. 2011). Bennett and Burau (2014) hypothesized a lateral tidal migration driven by tidally varying lateral turbidity gradients. In contrast, Rose et al. (2013) use salinity as the environmental cue guiding spawning migration. A previous modeling effort used a hybrid of salinity and turbidity cues to guide migration (RMA 2009). While several behaviors have been hypothesized and used in modeling studies, none of these studies contrast predicted distributions and entrainment resulting from different hypothesized behaviors. This comparison is the focus of this task of the CAMT delta smelt studies.

In this phase of modeling we aim to reproduce some general features of delta smelt distribution. One is retention in the northern estuary. Another is spatial distribution qualitatively consistent with Spring Kodiak Trawl observations. Lastly, we will compare the timing of predicted entrainment with the timing of observed salvage. The outcome of this comparison is an explanation and justification of behaviors that will be explored further in additional modeling work.

Simulation Periods

Two water years were chosen for this initial evaluation of behavior rules. Water year 2002 was chosen as a year with a clear signal in salvage and was simulated both with two-dimensional and three-dimensional modeling tools. Water year 2004 was chosen due to a double peak in observed salvage which is particularly challenging to reproduce with particle-tracking modeling. This report explores not only the relative performance of different behavior rules but also the predicted distribution by independent sets of modeling tools for 2002, a year in which both 2D and 3D tools are applied, and also the predicted distribution and entrainment during an additional water year (2004) using the 2D tools. An additional two years are considered for further evaluation of behavior rules by Korman et al. (2018).

Water year 2002 was classified as a dry year both on the Sacramento River and San Joaquin River (CDWR, 2016a). Prior to the spawning migration, delta smelt were observed primarily in the lower Sacramento River extending from Rio Vista down to the confluence in the Fall Midwater Trawl observations (Figure 1). Reported Net Delta Outflow (Figure 2) peaked at 105,892 ft^3s^{-1} on Jan 6, 2002 (CDWR, 2016b). The peak in salvage was observed on January 2, 2002 with a combined expanded salvage of 882 fish, which rapidly decreased as the magnitude of negative Old and Middle River flow decreased in early January.

The habitat of delta smelt was divided into regions for the CAMT investigations, primarily for the purpose of expanding catch into abundance and those regions, shown in Figure 3, are used here for comparison of observed and predicted regional abundance. Observed catch per unit effort in the Spring Kodiak Trawl (http://www.delta.dfg.ca.gov/data/skt) was expanded to estimate regional abundances as described in Korman et al. (2018). Estimated regional abundance based on the Spring Kodiak Trawl observations in 2002 (Figure 4) indicates a broader distribution than the Fall Midwater Trawl observations with delta smelt observed in the confluence and in Suisun Marsh.

Water year 2004 was classified as a below normal flow year on the Sacramento River and dry year on the San Joaquin River (CDWR, 2016a). Prior to the spawning migration the distribution of delta smelt was centered on the lower Sacramento River in and above the confluence (Figure 5). The peak flow of the year, 179,947 ft^3s^{-1}, occurred on Feb 28, 2004, unusually late in the water year, with a smaller flow peak on January 2, 2004 of 41,319 ft^3s^{-1} (Figure 6). Observed salvage also followed a dual peak with salvage ramping up at the time of each of the two flow peaks. The regional abundances estimated from

the 2004 Spring Kodiak Trawl surveys are shown in Figure 7. The possibility of variability in the sampling efficiency of the Spring Kodiak Trawl with turbidity is explored in Korman et al. (2018).

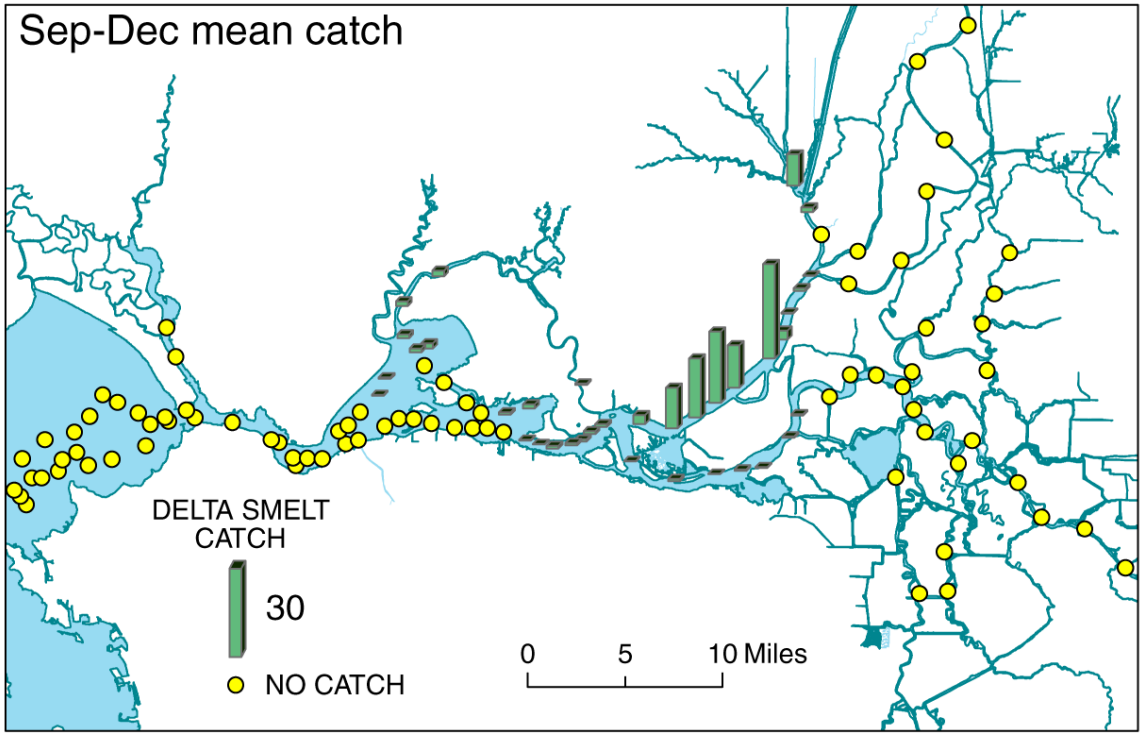

Figure 1**.** Observed mean catch per unit effort across all surveys of the 2001 Fall Midwater Trawl.

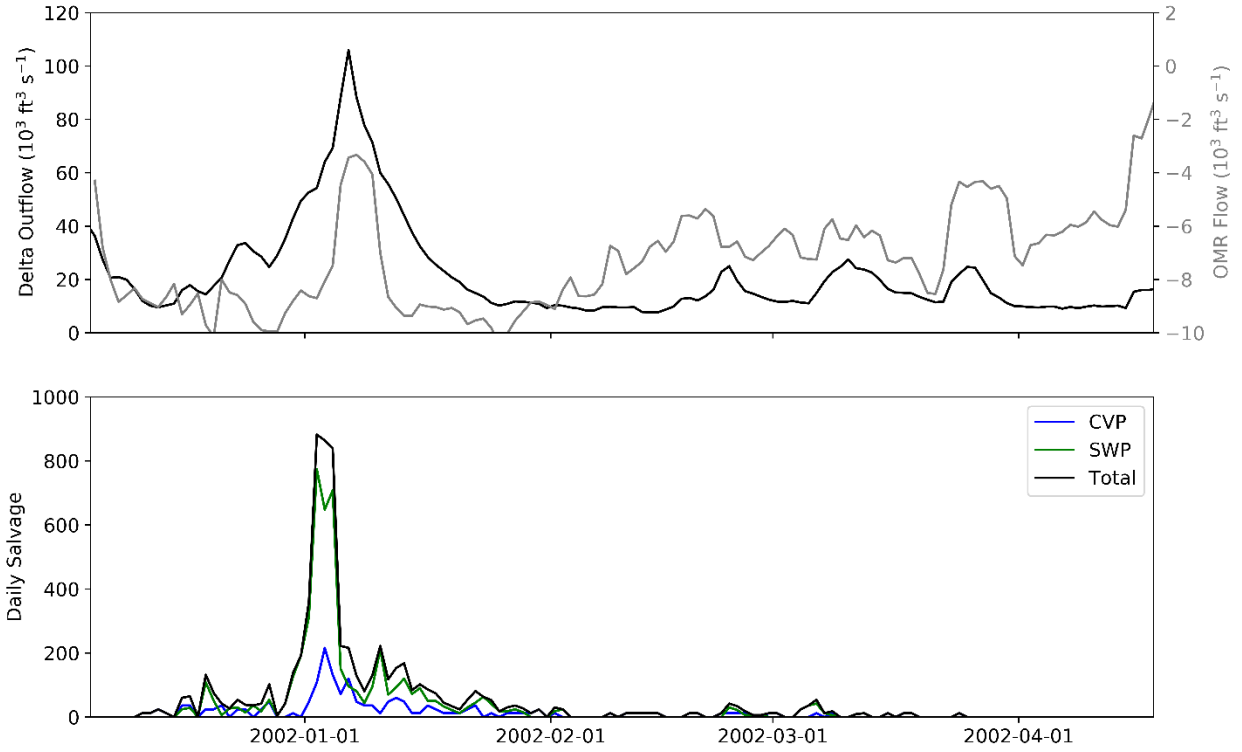

Figure 2**.** Net Delta outflow, OMR flow and expanded daily salvage during the water year 2002 simulation period.

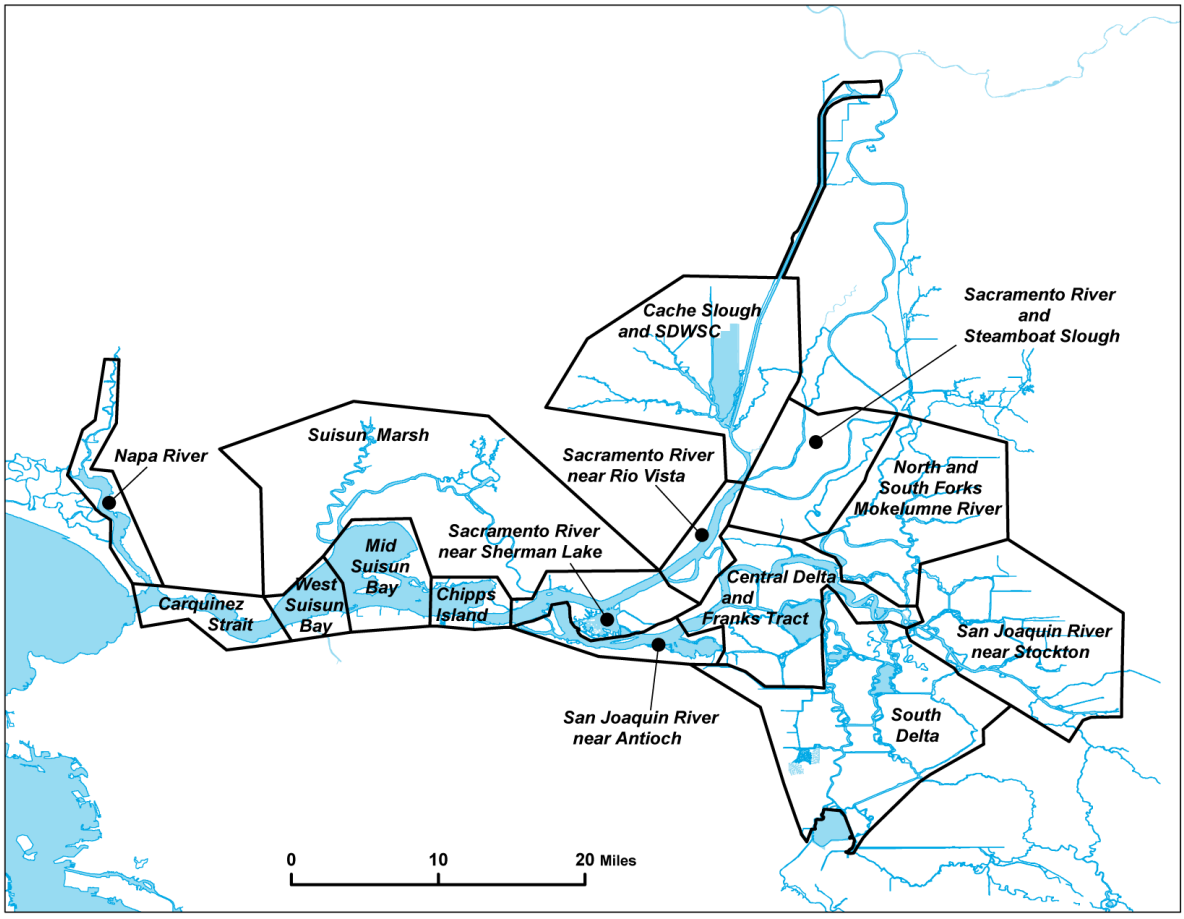

Figure 3**.** Regions used in CAMT delta smelt studies.

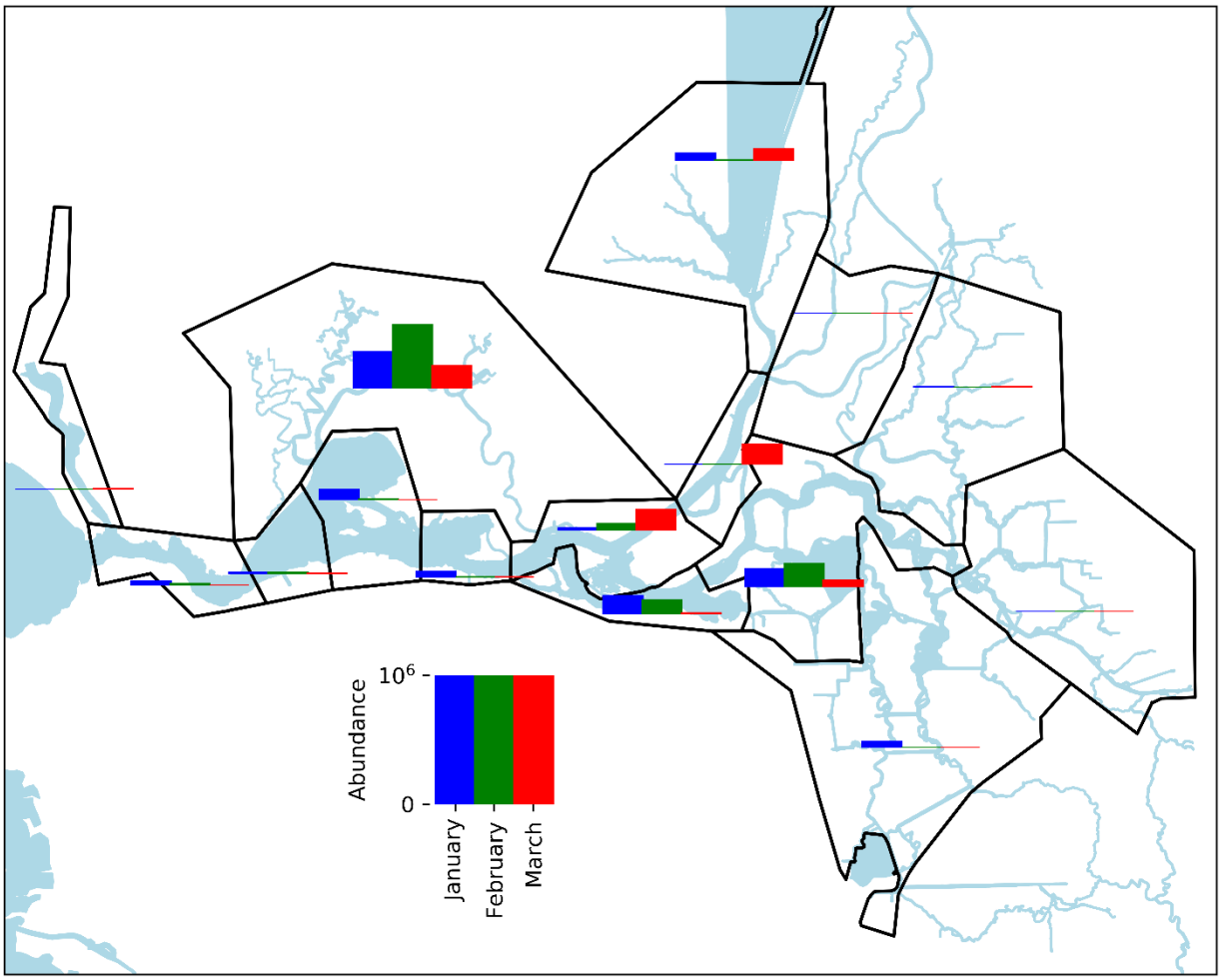

Figure 4. Estimated regional abundance for the three survey periods of the 2002 Spring Kodiak Trawl.

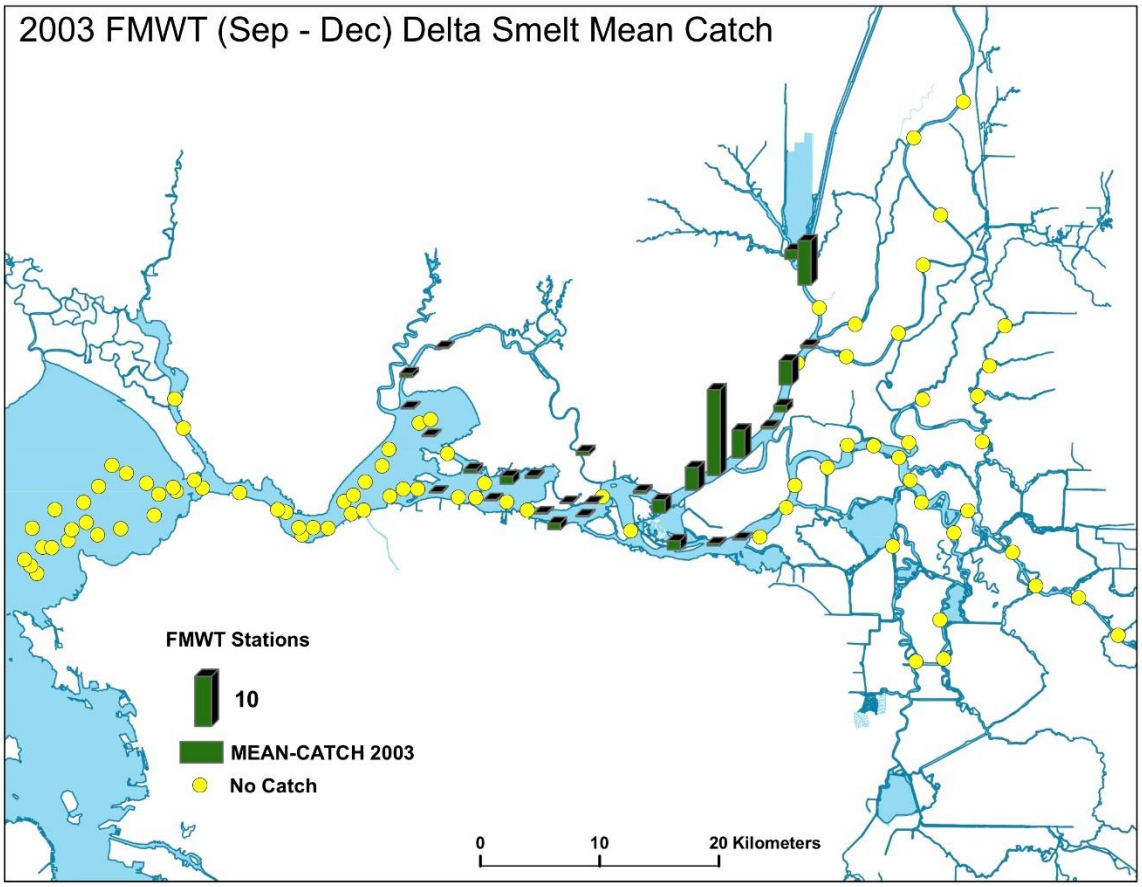

Figure 5. Observed mean catch per unit effort across all surveys of the 2001 Fall Midwater Trawl.

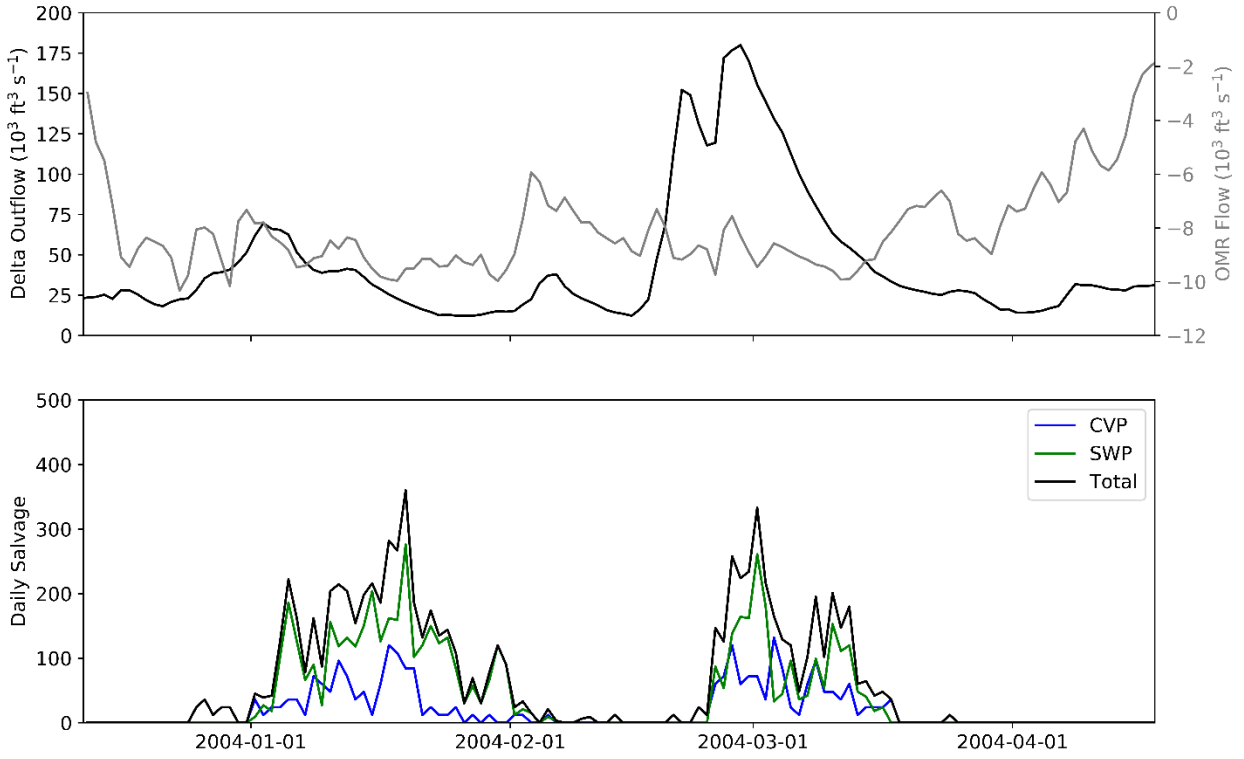

Figure 6. Net delta outflow, OMR flow and expanded daily salvage during the water year 2004 simulation period.

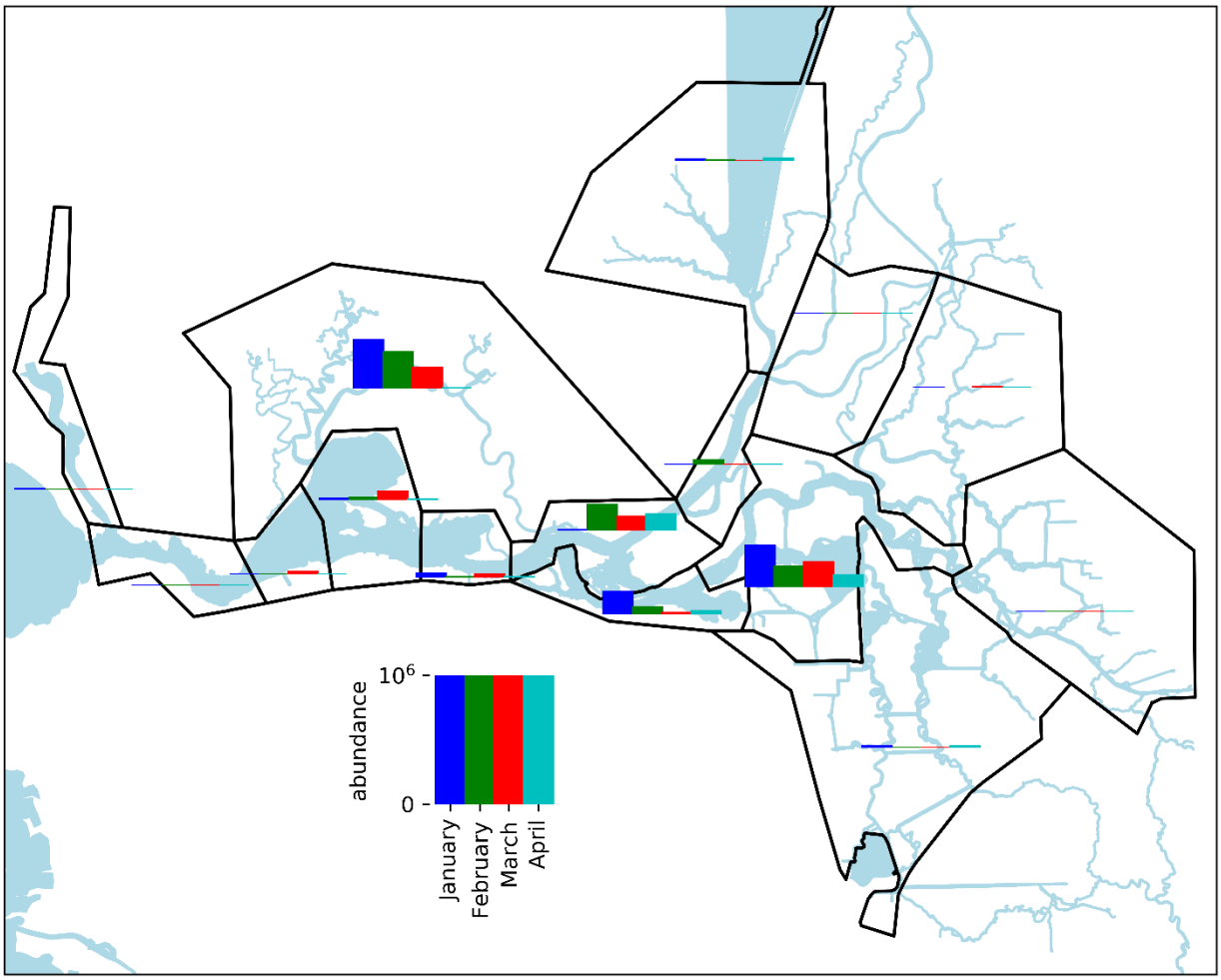

Figure 7. Estimated regional abundance for the four survey periods of the 2004 Spring Kodiak Trawl.

Hydrodynamic and Turbidity Modeling

Three-dimensional hydrodynamic, suspended sediment, and turbidity modeling was performed by Anchor QEA and builds on the hydrodynamic calibration documented in MacWilliams et al. (2015) and the suspended sediment calibration in Bever and MacWilliams (2013). The model calibration focused on water year 2011 when observations were available at several suspended sediment monitoring stations (Anchor QEA 2017).

Independent depth-averaged hydrodynamic, suspended sediment, and turbidity modeling was performed by RMA using RMA2 and associated tools. The calibration of these tools is documented in a report to CAMT (RMA 2017).

All hydrodynamic model output was written at a 15-minute output interval to be used in particle-tracking models.

Particle-Tracking Scenarios

The three-dimensional FISH-PTM model (Ketefian et al. 2016) was applied with the three-dimensional hydrodynamic output. The RMA-PTRK model (RMA 2009) was used applied with the two-dimensional hydrodynamic output. The initial particle distribution has been specified to approximate the observed 2001 Fall Midwater Trawl (FMWT) distribution shown in Figure 1. The distribution in the 2003 FMWT was similar.

Some attributes are consistent among simulations including release distribution in the lower Sacramento River and a simulation end time of the subsequent April 17 after the release time. The initial particle distribution with particles uniformly distributed through the Sacramento River near Sherman Lake and Sacramento River near Rio Vista regions is shown in Figure 8. The simulation end time of April 17 was chosen to include all Spring Kodiak Trawl surveys in both water year 2002 and 2004 and to include a period of zero salvage at the end of the simulation period. The attributes that vary among particle-tracking scenarios are:

1. Hydrodynamic modeling platform used
    a. 3D
    b. 2D
2. Water year of simulation period
    a. 2002
    b. 2004
3. Particle release time
    a. Water year 2002
        i. December 5, 2001
        ii. December 20, 2001
    b. Water year 2004
        i. December 12, 2003
4. Categories of behavior sets
    a. Passive
    b. Tidal migration
    c. Turbidity seeking
    d. Freshwater seeking
    e. Conditional tidal migration
    f. Compound behaviors

The particle release time of December 5, 2001 was chosen as the approximate time when elevated turbidity water reached the particle release region in 2002 (Figure 9). December 20, 2001 was chosen as the start time consistent with Sommer et al. (2011) determined by subtracting the reported time to reach SWP after the first flush (13 days) from the peak arrival of spawners at the SWP (January 2, 2002). The December 12, 2003 release time for water year 2004 was chosen to correspond with the arrival of elevated turbidity water in the lower Sacramento (Figure 10).

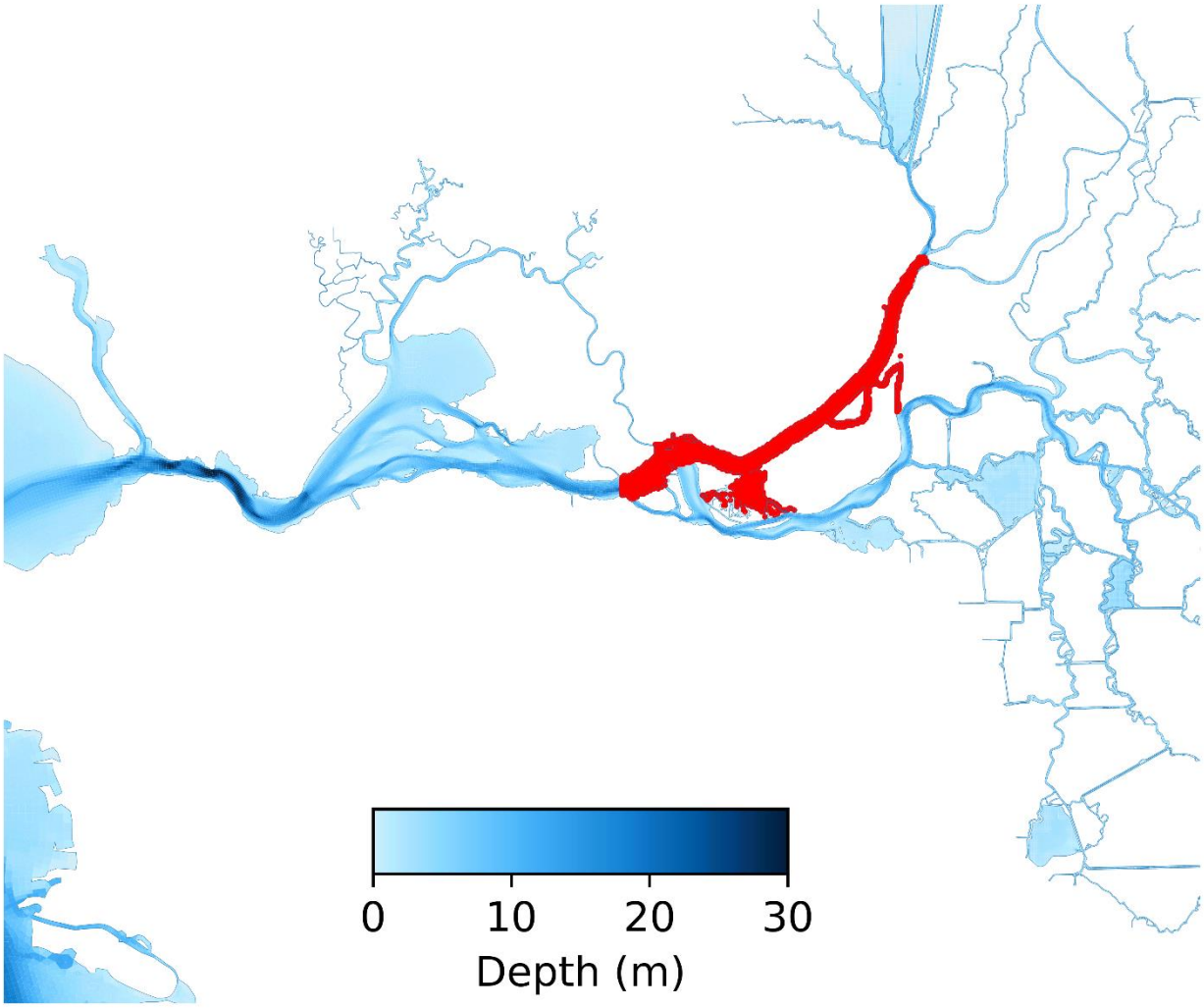

Figure 8. Initial distribution of particles at the particle release time. Each red dot indicates the horizontal position of a particle on December 5, 2001 at 00:00.

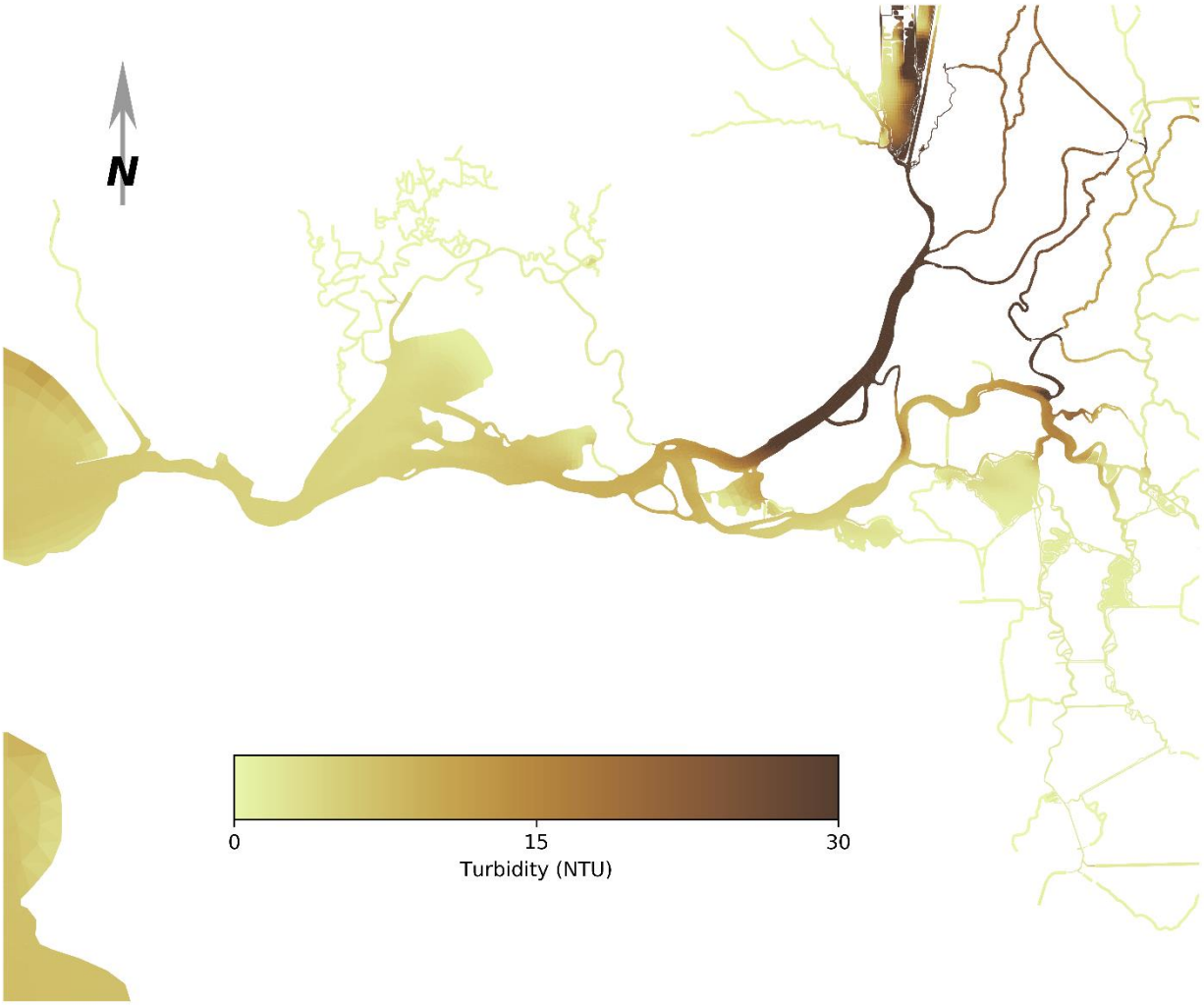

Figure 9. Depth-averaged turbidity field predicted by the 2D modeling tools on Dec 5, 2001 at 00:00.

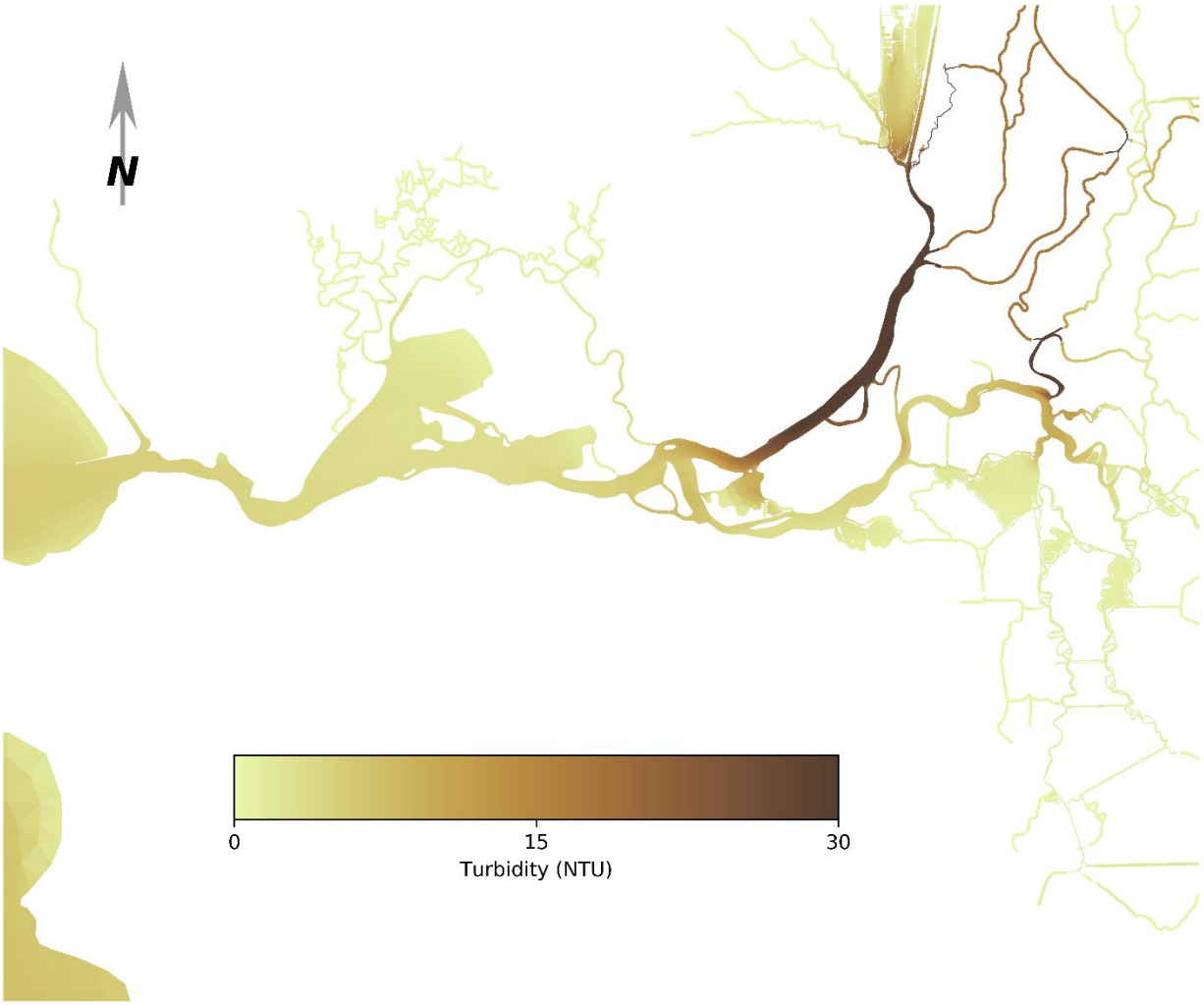

Figure 10. Depth-averaged turbidity field predicted by the 2D modeling tools on Dec 12, 2003 at 00:00.

Swimming Behavior Formulation

The hypothesized behavior rules were developed under guidance from the Delta Smelt Scoping Team (DSST) and based on review comments in the Independent Review Panel (IRP) review of the CAMT proposal for delta smelt investigations. However, given the limited observations available in this period and a potentially intractably large parameter space of a complex set of behavior rules, behaviors are explored within a specific framework. More complex variants of behavior, possibly involving additional environmental stimuli or stochasticity of responses, may be explored in the future if requested by the CAMT DSST.

Overview

All individuals (particles) are characterized by the state variables of three-dimensional position and swimming speed vector. Additional state variables associated with individuals, but only used in a subset of the behavior rules, are acclimated values of salinity and turbidity as explained below. The model proceeds in 5-minute time steps, so that state variables of each individual and the environmental stimuli

to which the individuals are exposed are updated at a 5-minute interval. The environmental stimuli are provided by the hydrodynamic models at the spatial resolution of the model grid which typically ranges from 10 meters to 100 meters through the Delta with smaller cell sizes in narrower channels. The instantaneous salinity and turbidity experienced by each individual at each time step are the turbidity and salinity in the grid cell containing the particle at that time step. Velocity is linearly interpolated through the cell according to the method of Ketefian et al. (2016). Gradients of salinity, turbidity and water depth are calculated from the values in the cell containing each particle and adjacent cells. The particle-tracking model accounts for movement of particles from the combination of hydrodynamics and swimming. The additional effect of natural mortality rate on predicted distribution is introduced in the statistical fitting subsequent to particle tracking.

Mathematical Formulation

The velocity of each particle/individual in the particle-tracking model is the summation of the hydrodynamic velocity vector and a swimming vector:

$$\vec{u} = \vec{u}_h + \vec{u}_b \tag{1}$$

where $\vec{u}_h$ is the hydrodynamic velocity and $\vec{u}_b$is the swimming (behavior) velocity specified by the individual-based model.

The swimming vector is specified as the summation of three orthogonal components of velocity and a horizontal component which can be in any direction in the horizontal plane:

$$\vec{u}_b = \vec{u}_s + \vec{u}_c + \vec{u}_v + \vec{u}_{xy} \tag{2}$$

where $\vec{u}_s$ is the streamwise swimming velocity, $\vec{u}_c$ is the cross-stream swimming velocity, $\vec{u}_v$ is the vertical swimming velocity, $\vec{u}_{xy}$ is the horizontal swimming velocity. The streamwise direction is defined as the direction of the hydrodynamic velocity at the location of the particle:

$$\vec{n}_s \equiv (n_x, n_y) = \frac{\vec{u}_h}{|\vec{u}_h|} \tag{3}$$

where $\vec{n}_s$ is the unit vector in the streamwise direction. By convention the positive cross-stream direction is to the right of the streamwise direction:

$$\vec{n}_c = (n_y, -n_x). \tag{4}$$

The direction of vertical swimming is by definition the z-coordinate direction:

$$\vec{u}_v = V(0,0,1) \tag{5}$$

where V is the vertical swimming speed and is positive for upward swimming.

Swimming speeds used vary to some extent but are generally limited to 2 body lengths per second or less. These are consistent with sustained swimming speeds reported by Swanson et al. (1998).

Behaviors are triggered by environmental stimuli at the location of each particle. Two types of environmental stimuli are considered. The first is the instantaneous and local value of an environmental property, such as turbidity or salinity. The second is a perceived change trigger based on change of an environmental property from an acclimatized condition (Goodwin et al. 2014). The acclimatized value of an environmental property is estimated based on a Pavlovian conditioning approach by an exponentially weighted moving average:

$$I_a(t) = (1 - m_a)I(t) + m_a I(t-1) \tag{6}$$

where $I_a(t)$ is the perceived intensity of an environmental stimulus I at time t, and m_a is a parameter which determines the time scale of acclimation. The perceived change is then the difference between the instantaneous value of an environmental stimulus and the acclimatized value of the stimulus is

$$E(t) = \frac{I(t) - I_a(t)}{I_a(t)} \tag{7}$$

The environmental properties that are considered as possible stimuli are discussed in the following section.

Based partially on input from the Delta Smelt Scoping Team, the behavior rules used in this study are intentionally of limited complexity and neglect several likely attributes of actual delta smelt behavior. There is no stochasticity in thresholds that trigger behavioral responses and no variability among particles in the swimming response to a given environmental stimulus. Furthermore, the behavioral rules do not change in time with life stage of delta smelt or with light levels (no variation between day and night behavior). The lack of change with life stage could be particularly limiting to the extent that delta smelt have a distinct staging behavior prior to spawning.

Behavior Triggers

The framework of triggers and associated behaviors allows a great deal of flexibility. However, there are also limitations, including the use of fixed thresholds to trigger behaviors.

The current types of triggers used in specified behaviors are of the following general types:

1. None: No condition required, used for a default behavior
2. Instantaneous: The instantaneous value of an environmental stimulus at the location of the particle is within a specified range, for example, turbidity > 15 NTU.
3. Gradient: The instantaneous value the gradient of an environmental property at the location of the particle is within a specified range, for example, turbidity gradient > 0.001 NTU/m.
4. Acclimatized (Equation 6): The acclimatized value of an environmental property is within a specified range, for example, the acclimatized salinity > 0.5 psu.
5. Perceived change (Equation 7): The perceived change from an acclimatized value of an environmental property is within a specified range, for example a (normalized) change in turbidity of 25%.
6. Timer: Used to attribute persistence to behaviors. For example, a tidal migration behavior could be specified to be active for a minimum of 24 hours once triggered.
7. Compound: Trigger types 2-6 can be combined to form compound triggers. For example, swimming to shallower water may be triggered when turbidity > 15 NTU and the hydrodynamic velocity at the particle location is in the ebb direction.

The environmental properties that have been considered in triggers of the general types described above include

1. Hydrodynamic velocity
2. Distance to shore
3. Water depth
4. Salinity
5. Turbidity

Each of these properties, and their gradients, are evaluated at the location of each particle and through time in the particle-tracking simulations.

Behavior Types

Triggers and associated behavioral (swimming) responses are combined to form sets of behavior rules. Several general types of swimming responses have been explored. Not only are triggers deterministic but all of the responses are deterministic. While there is currently no stochasticity in swimming response (swimming speed or direction) among individuals, it has been applied in the behavior representation of salmon (e.g. Goodwin et al. 2014) and could be explored in the future. The one exception is stochasticity in swimming direction for the "random" swimming behavior listed below.

1. Passive
    a. All swimming velocity components are zero
2. Turbidity seeking
    a. Swim in horizontal direction of higher turbidity
3. Freshwater seeking
    a. Swim in horizontal direction of lower salinity
4. Horizontal tidal migration
    a. Swim in horizontal direction to shallower water on ebb
    b. Swim in horizontal direction to deeper water on flood
5. Vertical tidal migration
    a. Swim down during ebb
    b. Swim up during flood
6. Holding
    a. Oppose/resist hydrodynamic velocity in the horizontal up to some threshold speed
    b. Swimming in horizontal direction shallow water when in deep water
7. Random
    a. Randomly directed swimming at a fixed speed

The direction of ebb tide is determined from an analysis of a single period in which the tidal water level is transitioning from higher high water to lower low water. The direction of the strongest velocity in each cell during this period gives the ebb direction for that location. Ebb tide at any location and time occurs when the dot product of the hydrodynamic velocity at that time and location with the ebb direction vector at that location (estimated by the aforementioned analysis) is positive. It is implicitly assumed in this approach that each individual can sense the ebb direction, though the mechanism through which this information is perceived is not known.

Evaluation of Predicted Distribution

Our population dynamics model predicts the abundance, distribution, survival, and entrainment of adult delta smelt on a daily time step. The model consists of process, observation, and likelihood (fitting) components. The process component predicts the abundance of the population in each of the 15 CAMT regions for each day of the simulation. The model uses the estimates of abundance in each region and the proportion of particles in that region that are entrained, as determined by the PTM, to predict the number entrained by day. The observation component of the model translates predictions into metrics which are observed by the Spring Kodiak Trawl surveys (SKT), and daily salvage at each fish collection

facility. The likelihood component compares predictions and observations to estimate process and observation parameters by maximizing the likelihood through non-linear search.

Simulation results from the PTM are summarized in an exchange or movement matrix $\mathbf{m_{i,d}}$, which is the cumulative proportion of the original particles that are present in region *i* on day *d*, or are entrained at each pumping facility (*i*=*k*). This exchange matrix is treated as a large set of fixed parameters by the population dynamics model. Predictions of abundance and entrainment from the population model are translated into trends in SKT catch over space and time and trends in salvage at each facility. These predictions are compared to data, and parameters are estimated by nonlinear search using a maximum likelihood approach. In the description of the population dynamics model which follows, Greek letters denote parameters that are estimated, upper case letters denote predicted state variables, and lowercase letters denote indices (not bold), or data (bold) or fixed parameters (bold).

The process component of the population dynamics model predicts the abundance of delta smelt adults by model day and region. Regional abundance depends on the initial total abundance and cumulative survival and movement, and is calculated from,

$$N_{i,d} = e^{\gamma} \cdot \prod_{d} \phi_d \cdot \mathbf{m}_{i,d} \tag{8}$$

where γ is the initial abundance in log space, ϕ is the estimated survival rate on day *d,* with the product of those rates up to day *d* (denoted by the ∏ symbol) being the cumulative survival from the start of the simulation to the end of day *d*, and $\mathbf{m_{i,d}}$ is the cumulative proportion of fish in a destination region or entrained. We do not allow survival rate to vary across regions in this analysis. However, as discussed below, additional mortality for particles that are entrained is captured in the estimate of the salvage expansion factor.

The natural survival rate of delta smelt is assumed to be constant over the duration of the simulations and is calculated from

$$\phi_d = \text{logit}\ (\alpha_o) \tag{9}$$

where logit() denotes that the value inside the parentheses is logit-transformed so $0 \leq \phi \leq 1$.

The cumulative number of fish entrained is calculated from,

$$N\_Ent_{k,d} = \sum_{i} N_{i,d=0} \cdot \prod_{d} \phi_d \cdot \mathbf{m}_{k,d} \tag{10}$$

where N_Ent is the number entrained from the start of the simulation through day *d* at pumping location *k*, and $\mathbf{m_{k,d}}$ is the cumulative proportion of fish entrained at pumping location *k*, as determined by the PTM. (10 scales the proportional entrainment rates from the PTM ($\mathbf{m_{k,d}}$) by accounting for initial abundance and losses due to natural mortality. The proportion of the initial population that is entrained at each pumping location up to and including day *d* is calculated from,

$$p\_Ent_{k,d} = 1 - \prod_{d} 1 - \frac{N\_Ent_{k,d} - N\_Ent_{k,d-1}}{\sum_{i} N_{i,d-1}} \tag{11}$$

(11) follows the same logic as Kimmerer (2008) and assumes natural and entrainment mortality are continuous processes over the duration of the model simulation. As a result, proportional entrainment on each day depends on the abundance at the end of the previous day, where that abundance in turn

depends on the initial abundances, and cumulative natural and entrainment losses. The ratio in Equation 11 is the proportion of fish entrained on day *d* from all regions relative to the total abundance (across all regions) at the end of the previous day. The term inside the product symbol (∏) is therefore the proportion of the population surviving entrainment on day *d*, and that product over days is the cumulative proportion surviving from the start of the simulation through day *d*. Entrainment losses include both pre-screen losses and direct losses to the pumps.

The observation model predicts SKT catch for each station and survey period from,

$$\hat{C}_{SKT_{s,d}} = N_{i(s),d} \cdot \theta_{SKT_{s,d}} \tag{12}$$

where, $\hat{C}_{SKT_{s,d}}$ is the predicted SKT catch at station *s* on day *d*, $N_{i(s),d}$ is the abundance in region *i* where station *s* is located (*i(s)*), and $\theta_{SKT_{s,d}}$ is the proportion of the population in region *i* sampled at station *s* on day *d*. This SKT sampling efficiency term is calculated from,

$$\theta_{SKT_{s,d}} = \theta_{c_{s,d}} \frac{\mathbf{vtow}_{s,d}}{\mathbf{vreg}_i} \tag{13}$$

where $\theta_{c_{s,d}}$ is an estimate of the proportion of smelt within the volume towed at a station that are captured (sampling efficiency), **vreg** is the volume of region *i* that delta smelt are distributed in, and **vtow** is the volume for the tow at station *s* sampled on day *d*. We assumed that delta smelt were evenly distributed to a maximum depth of 4 m (as in Kimmerer 2008). The proportion of smelt within the volume towed ($\theta_{c_{s,d}}$) was set to 1 for the analysis here.

Salvage in the population dynamics model is calculated from,

$$\hat{C}_{SAL_{k,d}} = (N\_Ent_{k,d} - N\_Ent_{k,d-1}) \cdot \theta_{S_{k,d}} \cdot \mathbf{p}_{\mathbf{S_k}} \tag{14}$$

where $\hat{C}_{SAL_{k,d}}$ is the predicted salvage on model day *d* at salvage location *k*, $\theta_{S_{k,d}}$ is the proportion of entrained fish that enter the salvage facility, and $\mathbf{p}_{\mathbf{S_k}}$ is the proportion of the flow in the salvage facility that is sampled per day. For consistency with past efforts, we refer to the inverse of salvage efficiency (θ_S^{-1}) as the salvage expansion factor. Time-specific values for $\mathbf{p_S}$ for each facility were not available for all relevant time periods, thus the observed daily salvage data available to us was already expanded to account for the proportion of volume sampled each day. By using expanded salvage observations, one is assuming that $\mathbf{p}_S$=1. However, when fitting the model, using expanded salvage data would overweight the importance of the salvage data relative to other data sources (SKT). To correct for this, $\mathbf{p_s}$ was set to a value that reflects the typical proportion of fish in the salvage facility that are sampled. Our results assume that $\mathbf{p_s}$=0.08 (sampling 10 minutes out of every two hours) for both facilities in all water years we simulated.

For the screening run evaluations, we assume salvage efficiency ($\theta_{S_{k,d}}$) can vary across facilities but does not vary over time,

$$\hat{C}_{SAL_{k,d}} = (N\_Ent_{k,d} - N\_Ent_{k,d-1}) \cdot \theta_{S_{k,d}} \cdot \mathbf{p}_{\mathbf{S_k}} \tag{15}$$

where λ_0 is the proportion of entrained fish that enter the salvage facility *k* on day *d* and are counted, in logit space.

The model is fit to the data by minimizing a negative log likelihood (NLL_{TOT}) that quantifies the combined fit of the model to SKT catch (NLL_{SKT}), and salvage data (NLL_{SAL}). The total negative log likelihood (NLL_{TOT}) is,

$$NLL_{TOT} = NLL_{SKT} + NLL_{SAL} \tag{16}$$

Each likelihood component is described below. Note that the total negative log likelihood only quantifies the discrepancy between predictions and observations (observation error). There is no component that penalizes process variation in population dynamics because that variation is not modelled. For example, we could have allowed daily survival rates to be drawn from a distribution where we estimated both the mean and the extent of variation. In data-limited situations it is not possible to separate process error from observation error. Including both would increase computational time considerably and would require informative priors on the extent of process or observation error, with total variance estimates conditional on those priors. We therefore use an 'observation error only' model (see Ahrestani et al. 2013).

We assume that the SKT surveys provide a reliable index of abundance over both space (across regions) and time (over SKT survey periods in a year). We assume that the capture probability of the SKT survey is known and is accurately determined by the scaling factors in Equation (12. SKT catch at each station and SKT survey period is assumed to be a random variable drawn from a negative binomial distribution (negbin),

$$NLL_{SKT} = -\sum_{s,d} \log(\, negbin(\mathbf{c}_{\mathbf{SKT}_{s,d}}, \hat{C}_{SKT_{s,d}}, \tau)) \tag{17}$$

where, NLL_{SKT} is the sum of negative log likelihoods across all sampling days (*d*) and stations (*s*), $\mathbf{c}_{\mathbf{SKT}_{s,d}}$ is the observed SKT catch by station and day, $\hat{C}_{SKT_{s,d}}$ is the predicted catch from Equation (12, and τ represents the extent of overdispersion in the data. To simulate greater belief in the SKT data, τ was set to 1 for the evaluations reported here. In this case the negative binomial distribution is equivalent to the Poisson, where the variance is equal to the mean. Our approach to modelling error in the SKT data is rather ad-hoc, but as discussed in Korman et a. (2018) there is insufficient information to accurately model it.

The observed salvage at each salvage location is assumed to be Poisson-distributed (pois) random variable,

$$NLL_{SAL} = -\sum_{k,d} \log(\, pois(\mathbf{c}_{\mathbf{SAL}_{k,d}} \cdot \mathbf{p}_{\mathbf{s}_k}, \hat{C}_{SAL_{k,d}})) \tag{18}$$

where, NLL_{SAL} is the sum of the negative log likelihoods across all days, $\mathbf{c}_{\mathbf{SAL}_{k,d}}$ is the reported expanded daily salvage at facility *k* on day *d*, $\mathbf{p}_{\mathbf{s}_k}$ is the average proportion of water that is sampled for fish at the salvage facility, and $\hat{C}_{SAL_{k,d}}$ is the predicted salvage computed from Equation (15. By including the proportion of water sampled for fish at the salvage facility for both observations (Equation (15) and predictions (Equation (12), approximately correct samples sizes are used in the likelihood.

Parameters of the model were estimated by maximum likelihood using nonlinear search in AD model-builder (ADMB, Fournier et al. 2011). We ensure convergence had occurred based on the gradients of change in parameter values relative to changes in the log likelihood and the condition of the Hessian matrix returned by ADMB. Asymptotic estimates of the standard error of parameter estimates at their maximum likelihood values were computed from the Hessian matrix within ADMB.

Results

Particle tracking results are provided for a set of scenarios. The categories of particle fate reported are entrained by exports, exited analysis region and retained in the northern estuary. Particles that are in or seaward of San Pablo are considered to have exited the analysis region.

Each set of behavior rules ("behavior set") explored in this report is described in Appendix A. A full set of figures for 3D and 2D model results for each behavior set is provided in Appendix B.

Building from Simple to More Complex Behavior Sets

In this discussion the outcome of simple behavior rules is discussed first. For example, passive behavior is discussed as a reminder that some form of behavior is required for retention in the estuary and to quantify how quickly particles are lost out of the northern estuary without active behavior. Then active behaviors that are constant through time are explored. Next active behaviors that are only triggered under specific environmental conditions are explored. Last, behaviors with more than one possible behavioral response are discussed. The results shown here are a subset of the full set of results given in Appendix B.

Two figure types are used in the discussion of different hypothesized sets of behavior rules. Map figures have been prepared to compare the observed and predicted regional abundance at the time of the Spring Kodiak Trawl (e.g. Figure 12). Time series comparisons show the fate of the group of particles through time, classified into the categories of retained in the analysis region, which corresponds to the spatial region in which adult delta smelt are typically observed, exited from that region, or entrained into water exports (Figure 11). A time series of the proportion of particles exhibiting different categories of behavior through time (tidal migration, holding, etc.) is also shown. Next the timing of observed salvage is compared with the timing of particle entrainment. It should be noted that the particle entrainment does not consider natural mortality so this comparison is purely qualitative. Lastly, for reference, time series of Net Delta Outflow and Old and Middle River flow are shown.

For many behavior sets the two-dimensional and three-dimensional results are broadly similar, though often different in some individual regions. In the discussion below, primarily the three-dimensional results are shown but the full set of results for both 3D and 2D modeling tools are given in Appendix B. All behavior scenarios for both the 2D and 3D models for 2002 and 2D model for 2004 are included in the ranking of behaviors which will be discussed after the following discussion of results for individual behavior scenarios.

Passive Particles

Passive particles provide a useful reference of the outcome of plankton that are transported passively with the water. Figure 11 indicates that passive particles rapidly exit the northern estuary as they are

flushed to the ocean in both the 2D and 3D model results. The fitting approach selects the maximum allowable initial population of 5 million delta smelt to offset large seaward losses. Entrainment is relatively small compared with seaward losses.

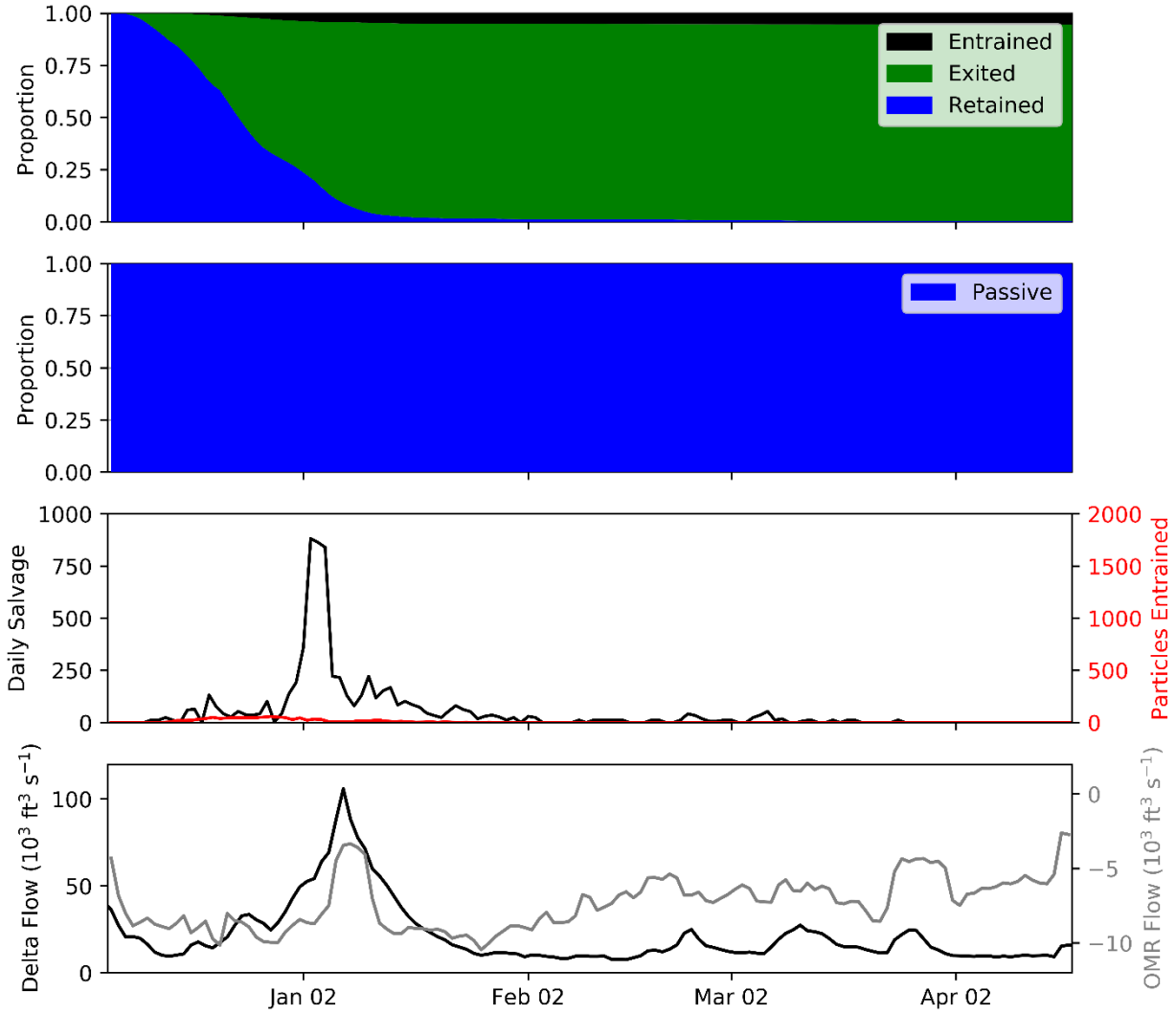

Figure 11. Passive behavior scenario results, three-dimensional model, water year 2002. The top panel shows the proportional fate of the particles through time, classified into the categories of retained in the analysis region, which corresponds to the spatial region in which adult delta smelt are typically observed, exited that region, or entrained into water exports. The second panel shows the proportion of particles exhibiting different types of behavior through time. The third panel shows daily expanded salvage and daily particle entrainment. The last panel shows daily Net Delta Outflow and Old and Middle River flow.

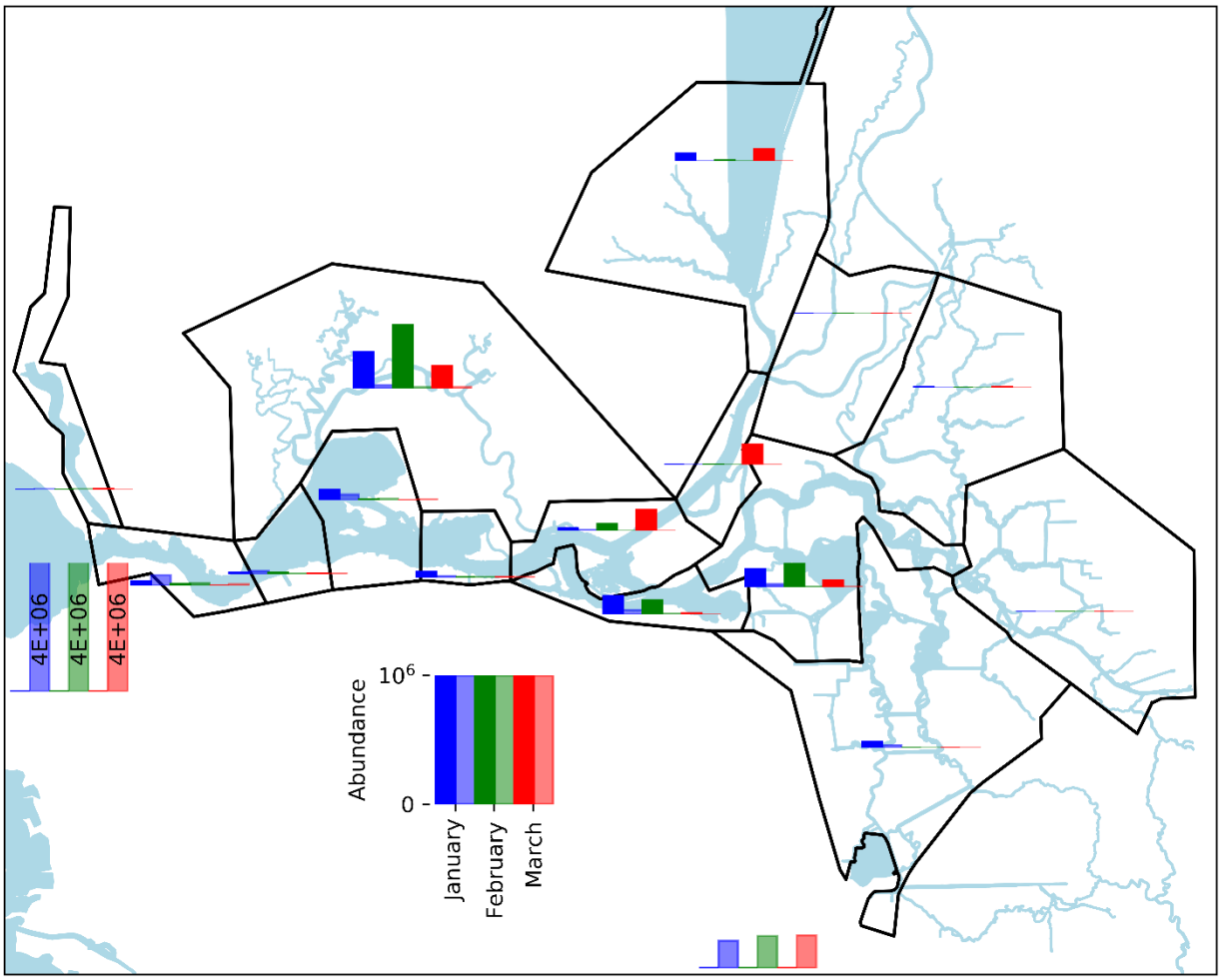

Figure 12. Comparison of predicted regional abundance for the passive behavior scenario, three-dimensional model results, water year 2002 to regional abundance estimated from the Spring Kodiak Trawl surveys. Dark colors for each month represent regional abundance estimated from each Spring Kodiak Trawl survey in 2002. Lighter colors for each month indicate model results. The predicted proportion of fish that exited the analysis region are shown to the left and below the Carquinez Strait region. Predicted cumulative entrainment is shown by the southernmost set of bars. The maximum height of each bar corresponds to a regional abundance of 10^6 delta smelt as shown in the legend. In cases where a predicted regional abundance of 10^6 delta smelt exceeded, the predicted regional abundance is annotated inside the corresponding bar.

Horizontal Tidal Migration

Tidal migration is implemented as horizontal swimming in the direction of shallow water (to the shoreline) on ebb and in the direction of deeper water (to the channel) during flood. Swimming speed for this behavior and most others is set at 8 cm s^{-1} which is approximately 1.5 body lengths per second for adult delta smelt. Vertical tidal migration was also explored using the 3D PTM, but found to be less effective at retaining particles in the freshwater (unstratified) portion of the estuary and not carried forward into the scenarios documented here.

The specified horizontal tidal migration behavior is effective at retaining particles in the estuary, as shown in Figure 13. However, it tends to move particles far landward and primarily into regions without large net river flow. This leads to large predicted entrainment losses and poor comparison to catch distribution observed in the Spring Kodiak Trawl surveys (Figure 14).

This outcome of this simple tidal migration behavior scenario can be understood to be the opposite extreme of the passive results because the passive scenario the particle distribution shifts strongly in the seaward direction while the tidal migration scenario results in a strong shift in the landward direction exposing particles to entrainment losses.

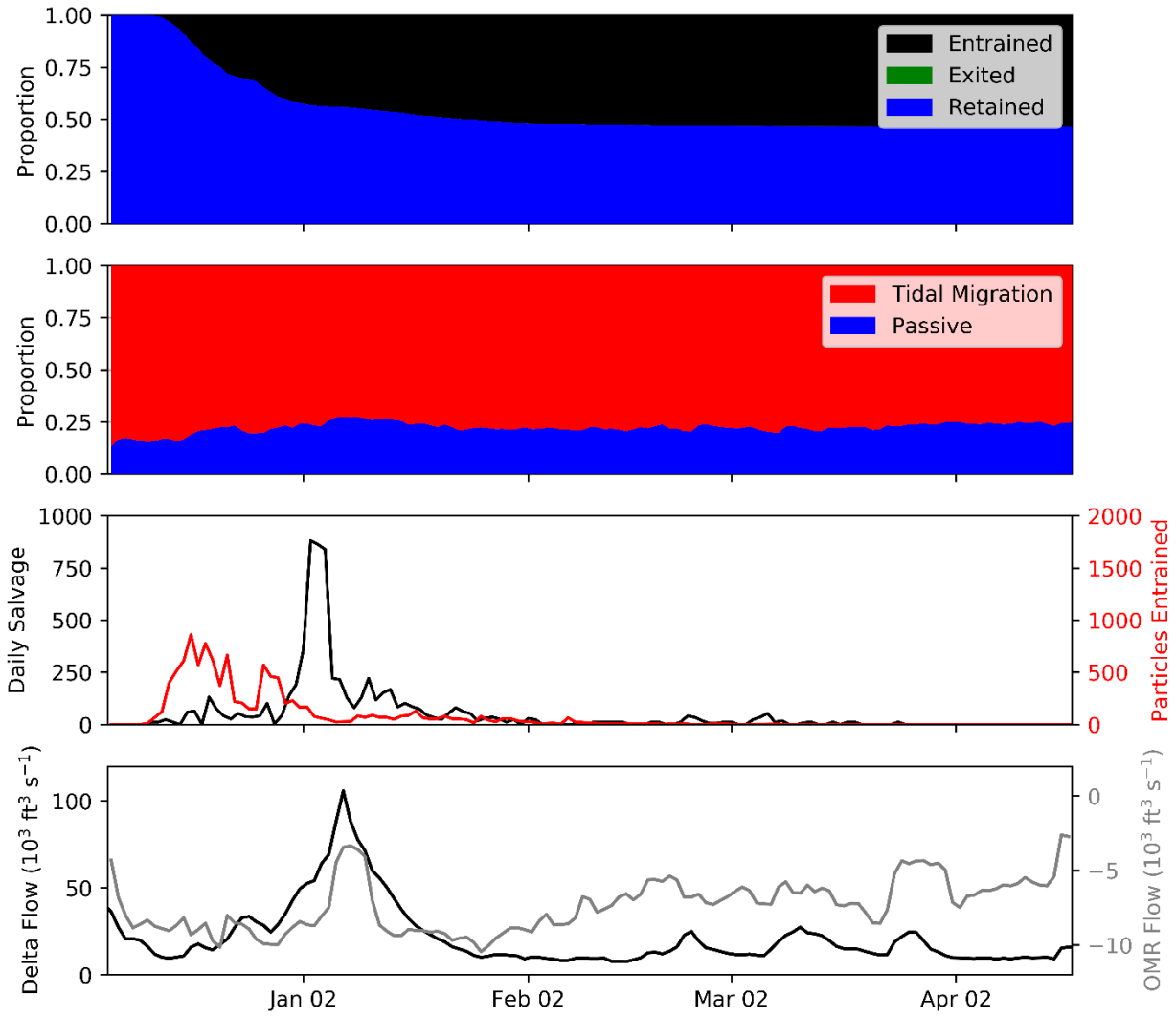

Figure 13. Tidal migration behavior scenario results, three-dimensional model, water year 2002. See caption for Figure 11.

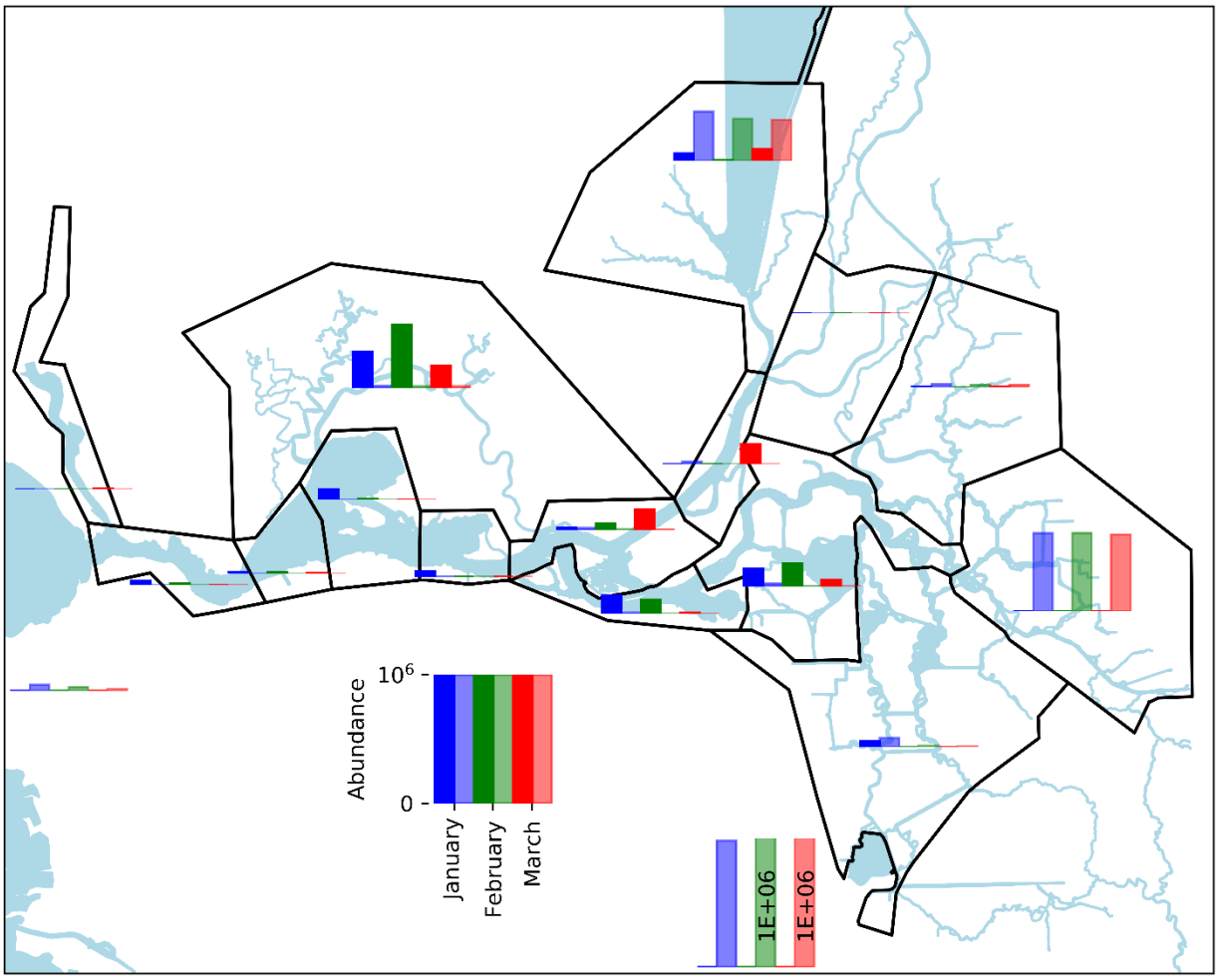

Figure 14. Comparison of predicted regional abundance for the tidal migration behavior scenario, three-dimensional model results, water year 2002 to regional abundance estimated from the Spring Kodiak Trawl surveys. See caption for Figure 12.

Turbidity Seeking

The simple turbidity seeking behavior explored is defined as horizontal swimming in the direction of the positive turbidity gradient. Turbidity seeking behavior results in poor retention, as shown in Figure 15. In the three-dimensional model results some particles are retained in Suisun Marsh (Figure 16), possibly due to weak net velocities through Suisun Marsh and a persistent orientation of turbidity increasing to the eastern (landward) side of Montezuma Slough. Fewer particles are retained in Suisun Marsh in the 2D model results (Figure 16). Turbidity seeking results in minimal entrainment for both models.

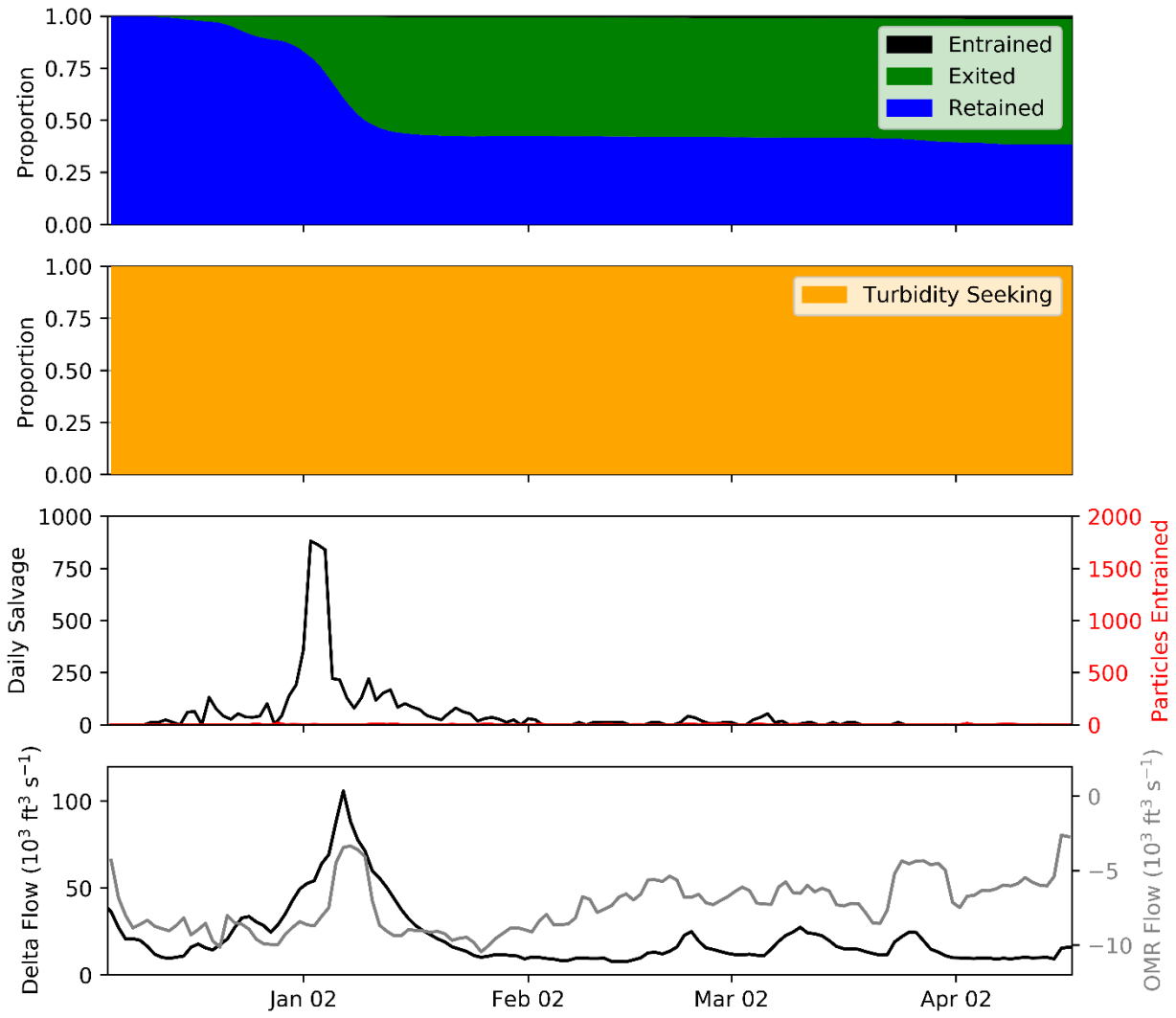

Figure 15. Turbidity seeking behavior scenario results, three-dimensional model, water year 2002. See caption for Figure 11.

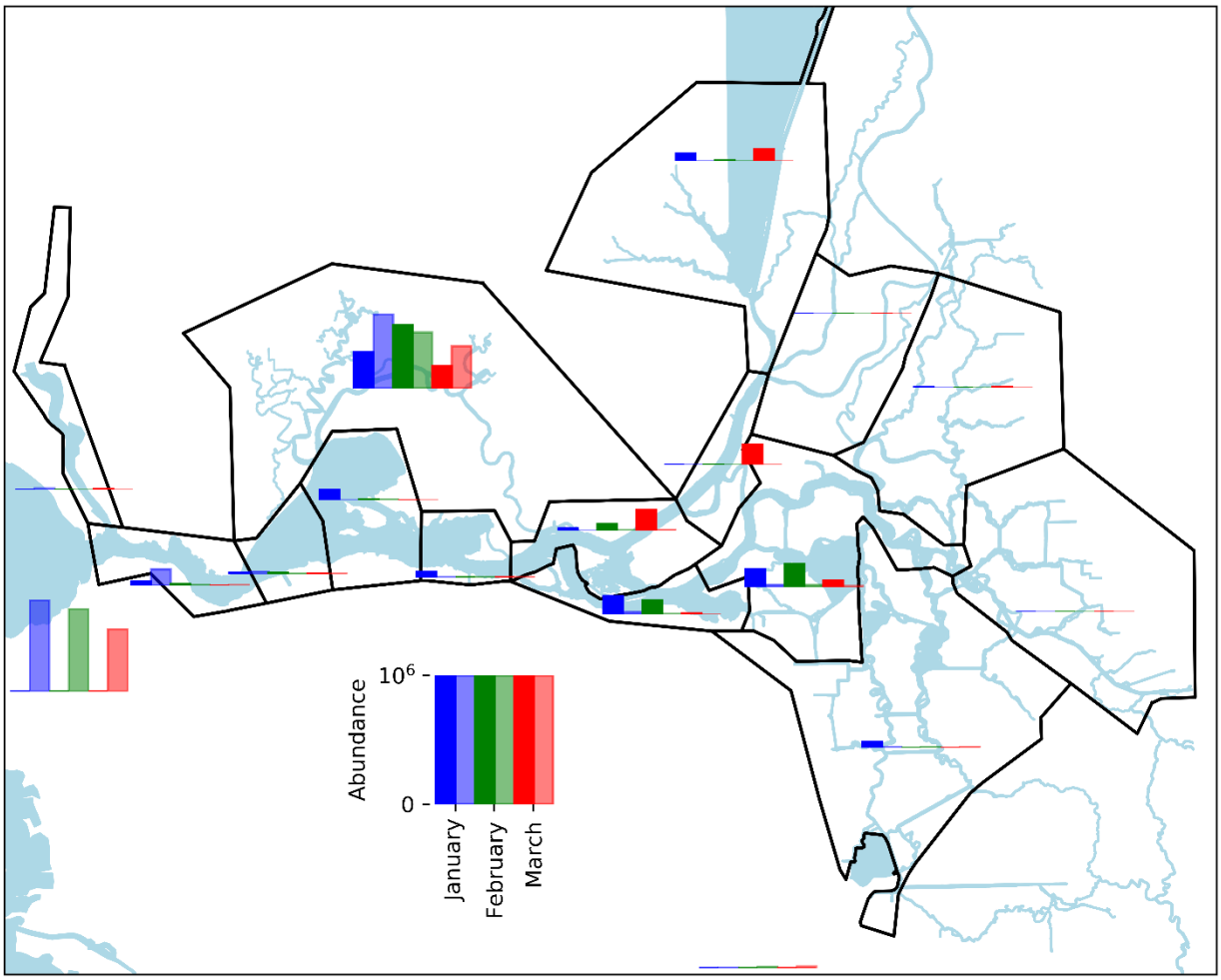

Figure 16. Comparison of predicted regional abundance for the turbidity seeking behavior scenario, three-dimensional model results, water year 2002 to regional abundance estimated from the Spring Kodiak Trawl surveys. See caption for Figure 12.

Freshwater Seeking

Freshwater seeking behavior is defined here as horizontal swimming in the opposite direction of the salinity gradient. Similar to turbidity seeking, freshwater seeking leads to poor retention and low entrainment in all simulations (Figure 17). Freshwater seeking does not retain particles as effectively in Suisun Marsh as turbidity seeking (Figure 18).

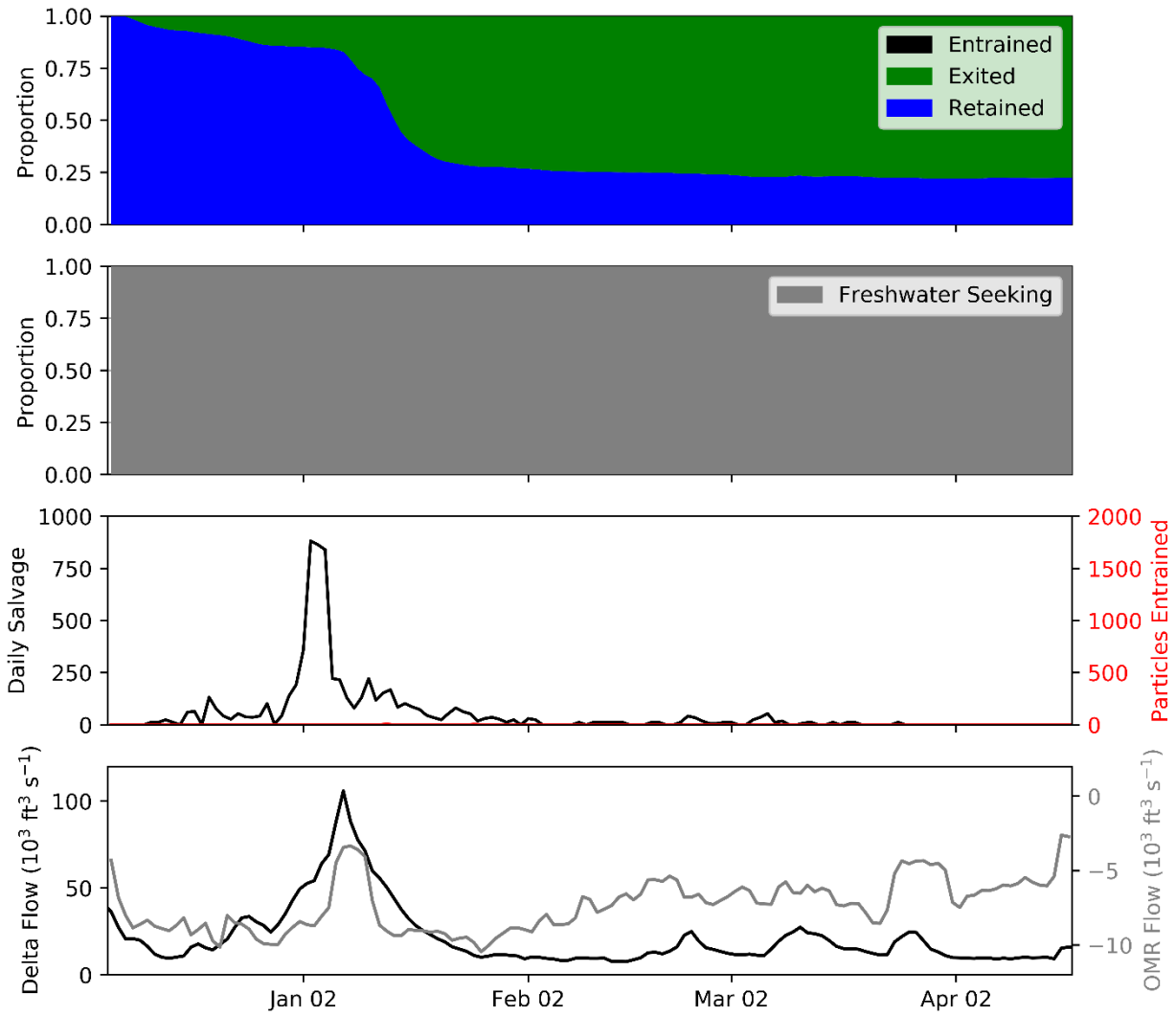

Figure 17. Freshwater seeking behavior scenario results, three-dimensional model, water year 2002. See caption for Figure 11.

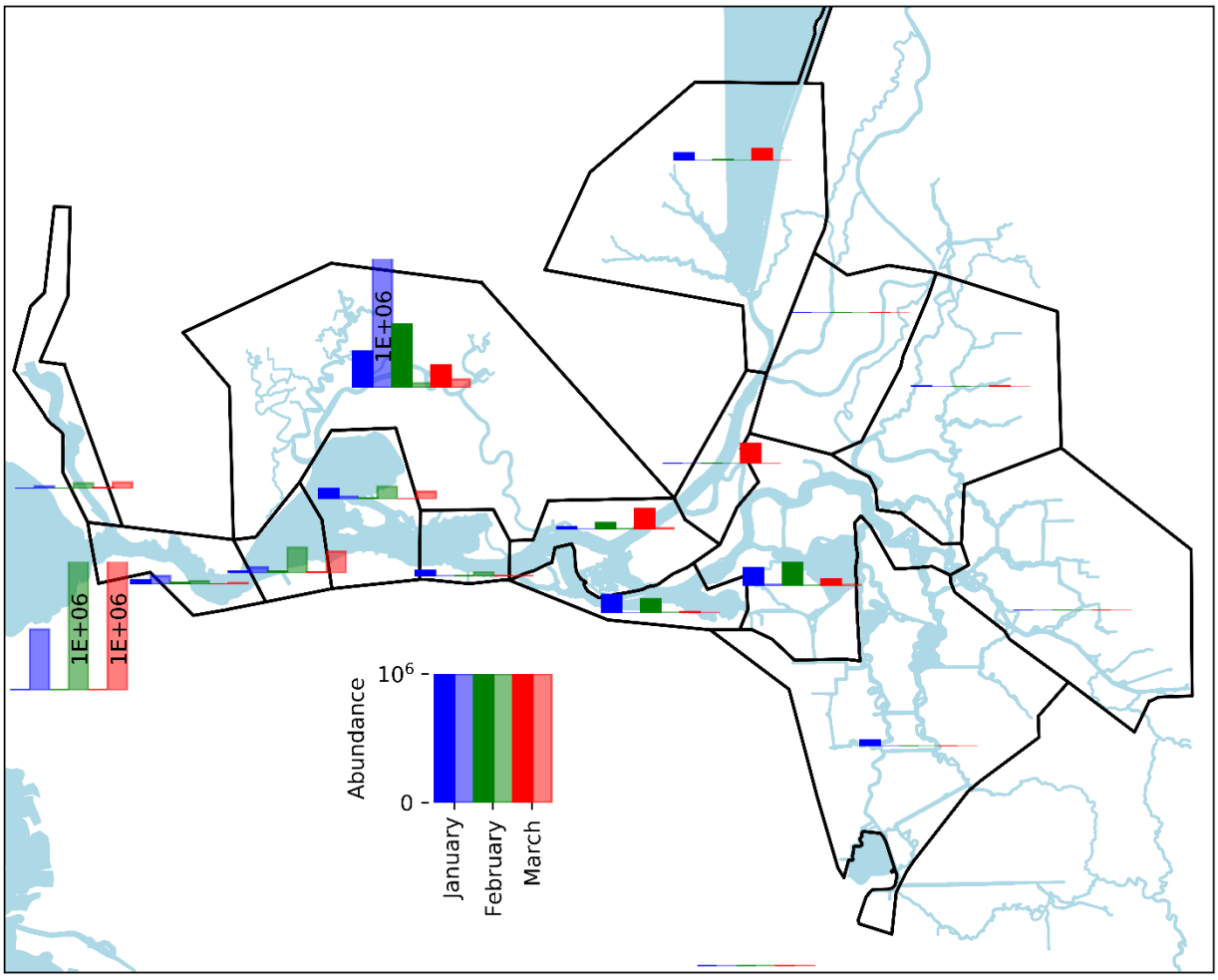

Figure 18. Comparison of predicted regional abundance for the freshwater seeking behavior scenario, three-dimensional model results, water year 2002 to regional abundance estimated from the Spring Kodiak Trawl surveys. See caption for Figure 12.

Conditional Tidal Migration

The simple behaviors explored so far are essentially continuous through the entire simulation period. Though not shown in this report, several more complex variations of these behaviors have been explored, but did not provide substantially improved results. The remaining scenarios reported all involve some form of conditional tidal migration, meaning that tidal migration is performed only under certain environmental conditions. In several cases conditional tidal migration is combined with other behaviors such as holding behaviors. A full set of figures for all behavior sets is provided in Appendix B. Here we will describe the incremental effect of several different aspects of behavior.

A conceptual model of some previous delta smelt studies was tidal migration only in turbid water and, therefore, a “turbidity bridge” would be required to move a substantial portion of delta smelt into the interior Delta against net seaward flows (RMA 2009). In Figure 19 the effect of making tidal migration conditional on turbidity with a threshold of 12 NTU is shown. The application of the turbidity threshold results in substantially less tidal migration yet a higher proportion of particles are entrained. This may be counter intuitive but can be explained by Figure 14 which shows that for continual tidal migration a

portion of the particles move to landward reaches of the domain such as Cache Slough and the San Joaquin River near Stockton. Those particles escape entrainment. However, the conditional tidal migration behavior keeps more particles in the central Delta in January where they are prone to entrainment (Figure 20). The results are not substantially changed by applying a higher turbidity threshold of 18 NTU (Figure 21).

An alternative to turbidity as the primary condition to regulate tidal migration behavior is salinity. Performing tidal migration only when salinity exceeds 1 psu results in greatly reduced entrainment relative to continuous tidal migration (Figure 22). This is understandable because high salinity did not intrude into the Delta in this period so tidal migration only in brackish water did not put many particles at risk of entrainment but was adequate to retain particles in the analysis region. A variation on this behavior is persistent tidal migration in brackish water in which tidal migration persists for at least 12 hours when triggered. The persistence results in slightly improved retention and slightly increased entrainment as shown in Figure 23.

An alternative trigger to initiate persistent tidal migration is perceived salinity change that is triggered when the salinity experienced by the particle is increasing through time. This preceived change trigger may be expected to have somewhat similar behavior to tidal migration in high salinity because it is also likely to be triggered as particles move seaward into more saline regions. However, since it is a proportional change metric in which the change is normalized by the acclimatized salinity experienced by the particle, it can also be triggered by local salinity gradients in regions with salinity less than 1 psu. Therefore, it is more likely to trigger in the interior Delta than the salinity greater than 1 psu trigger. As shown in Figure 24, both behaviors are effective at retaining particles and the trigger associated with increasing salinity leads to higher entrainment because it is more likely to be triggered in landward regions.

As will be seen in the next section on ranking particles, the best performing behaviors generally consist of conditional tidal migration with some form of salinity based trigger in conjunction with conditional holding or another additional behavior type. The effect of the addition of a holding type behavior to the tidal migration in perceived increasing salinity behavior is shown in Figure 25. The addition of holding reduced predicted entrainment in that case, though not in all cases in which holding was applied (see results in Appendix B).

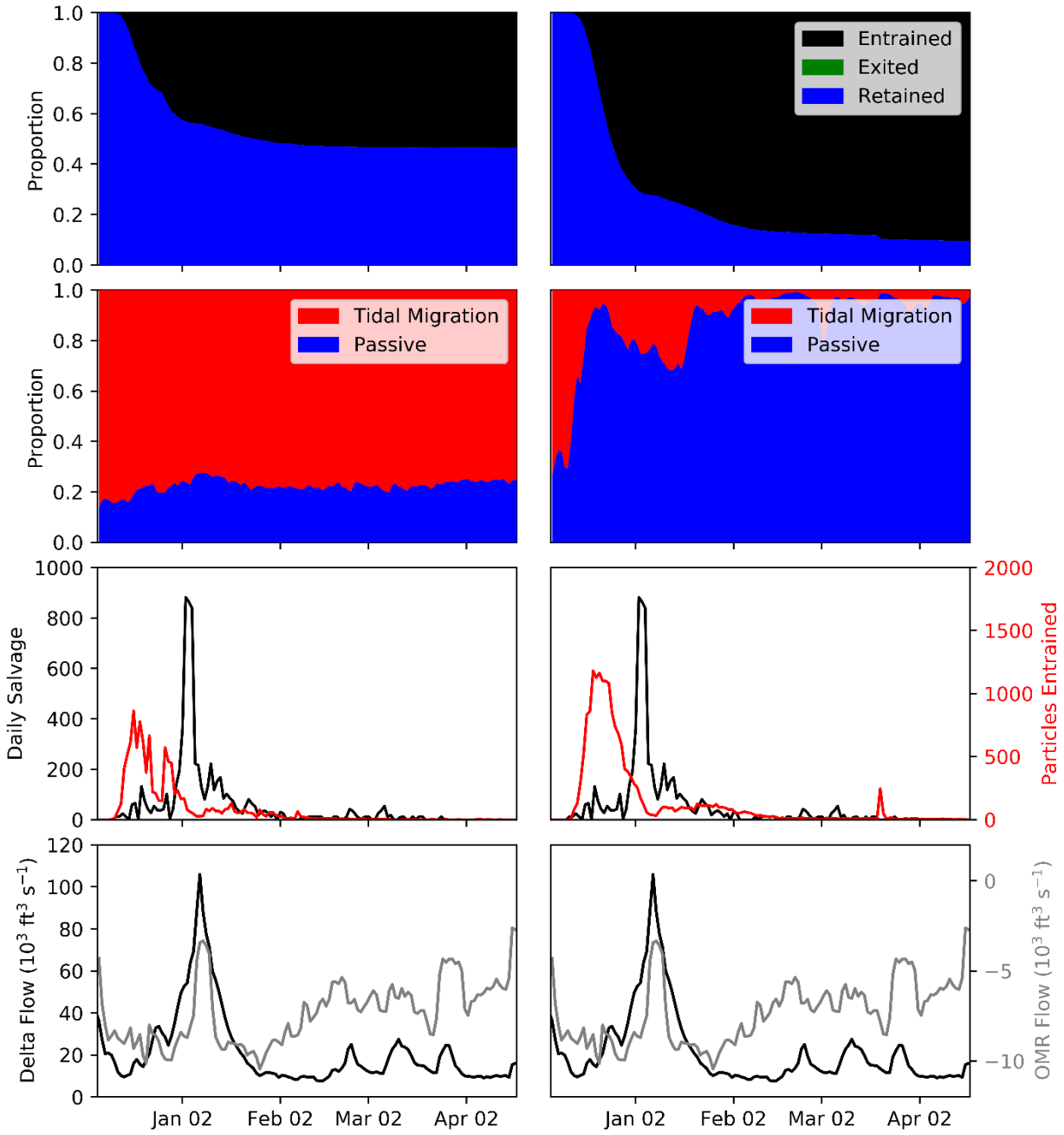

Figure 19. Results of tidal migration behavior set (left panel) and tidal migration in turbid water only behavior set (right panel) for three-dimensional model, water year 2002. See caption for Figure 11.

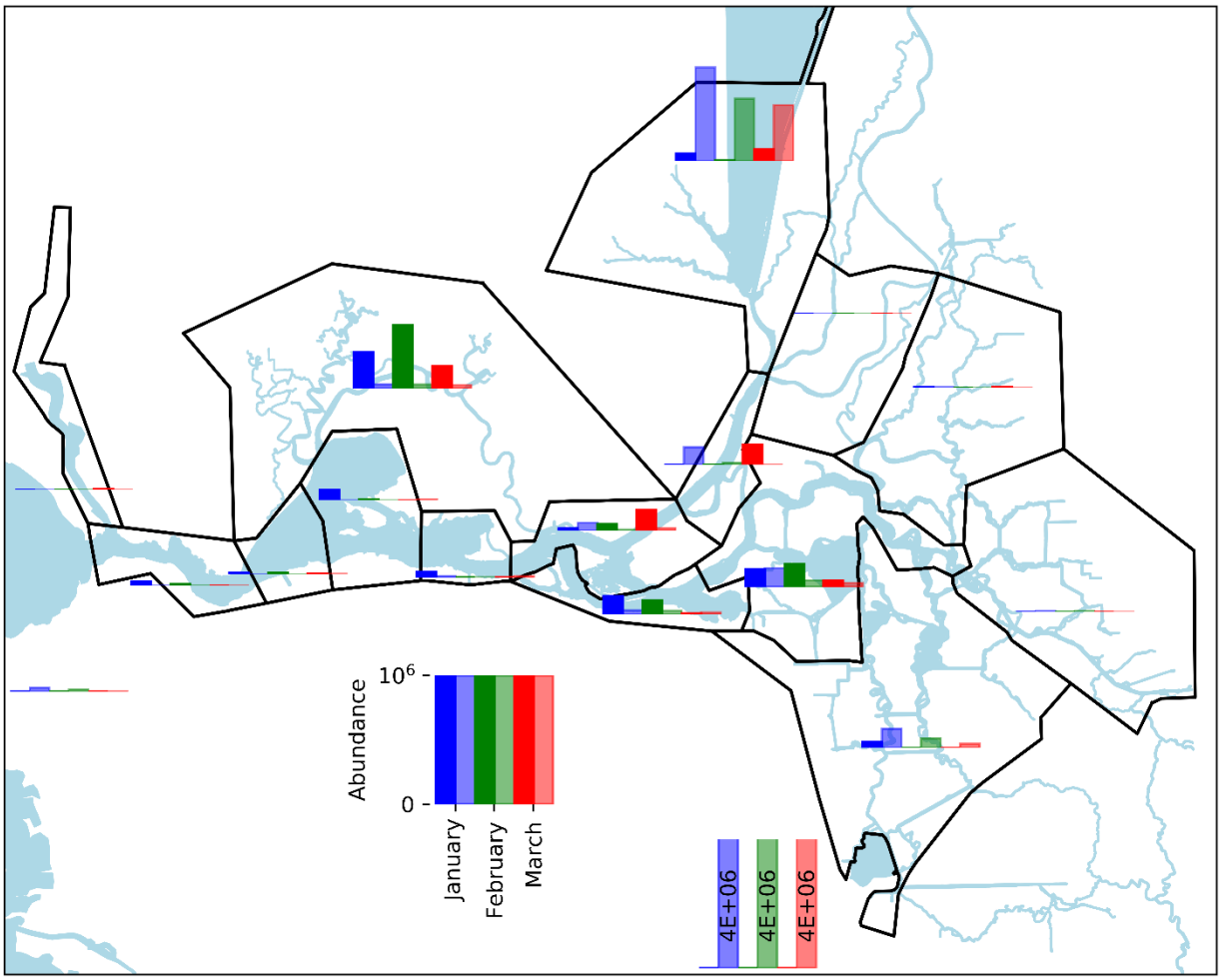

Figure 20. Comparison of predicted regional abundance for the turbidity seeking in turbid water behavior set, three-dimensional model results, water year 2002 to regional abundance estimated from the Spring Kodiak Trawl surveys. See caption for Figure 12.

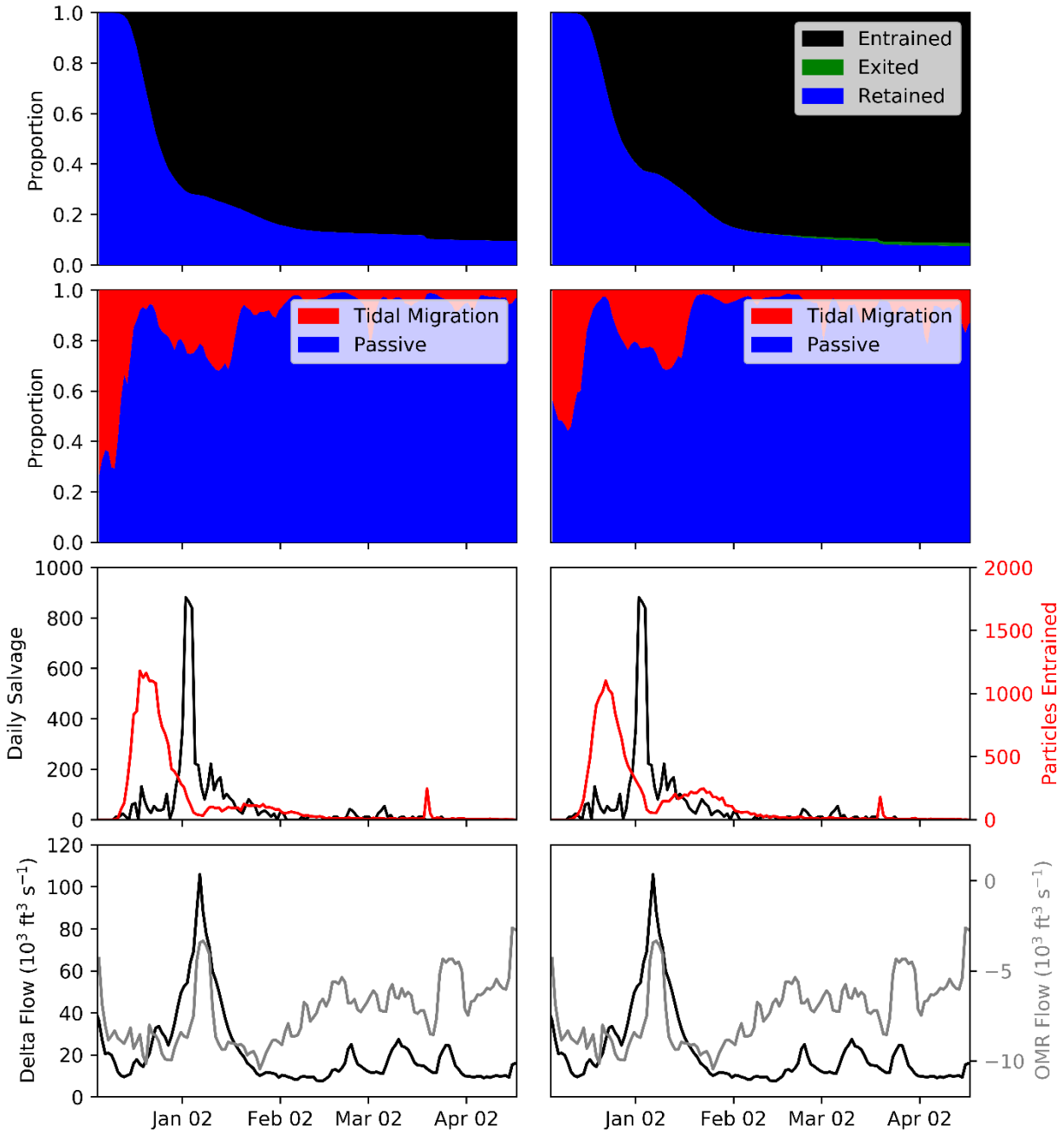

Figure 21. Results of tidal migration in turbid water behavior set (left panel) and tidal migration in highly turbid water behavior set (right panel) for three-dimensional model, water year 2002. See caption for Figure 11.

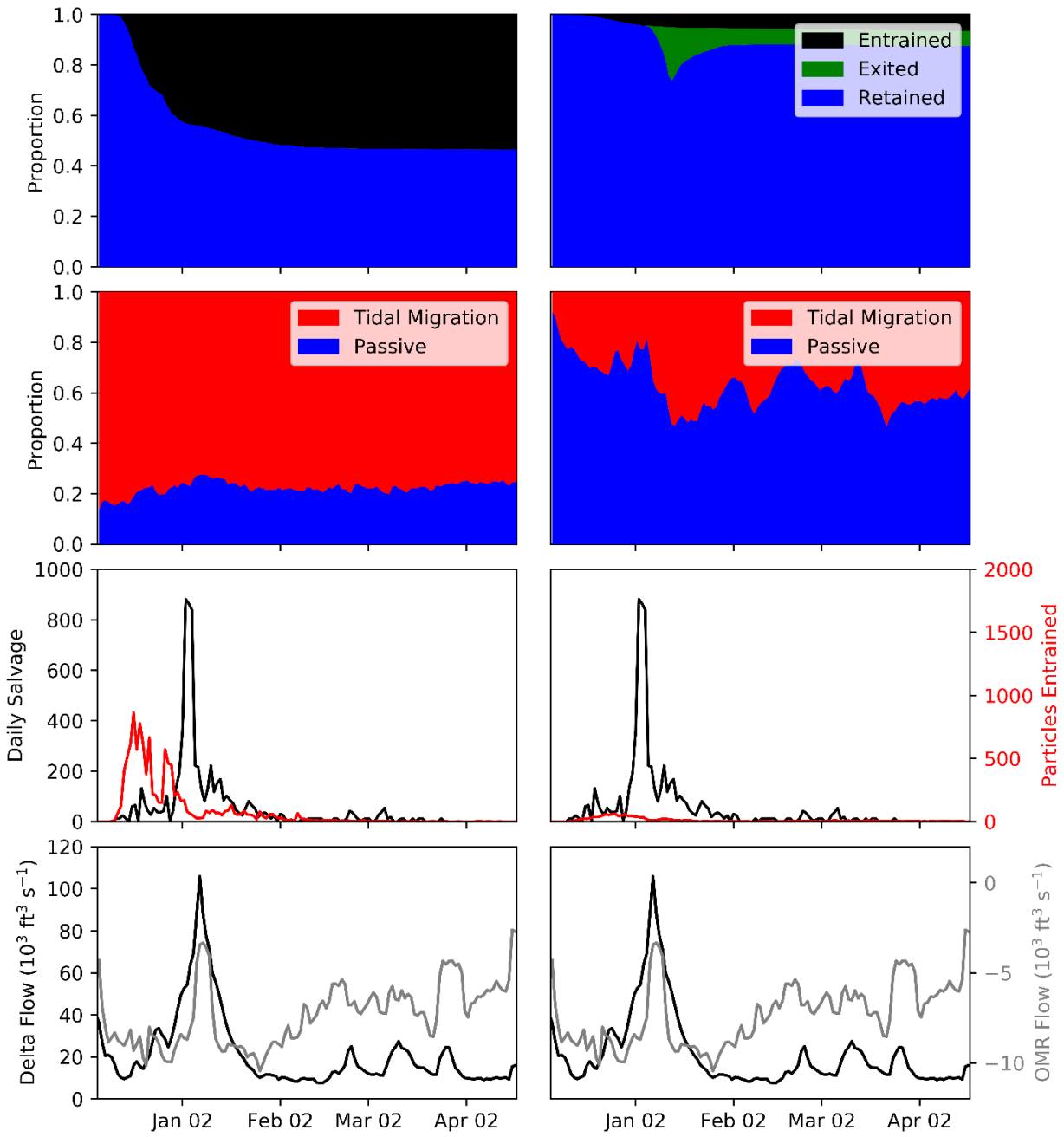

Figure 22. Results of tidal migration behavior set (left panel) and tidal migration in brackish water behavior set (right panel) for three-dimensional model, water year 2002. See caption for Figure 11.

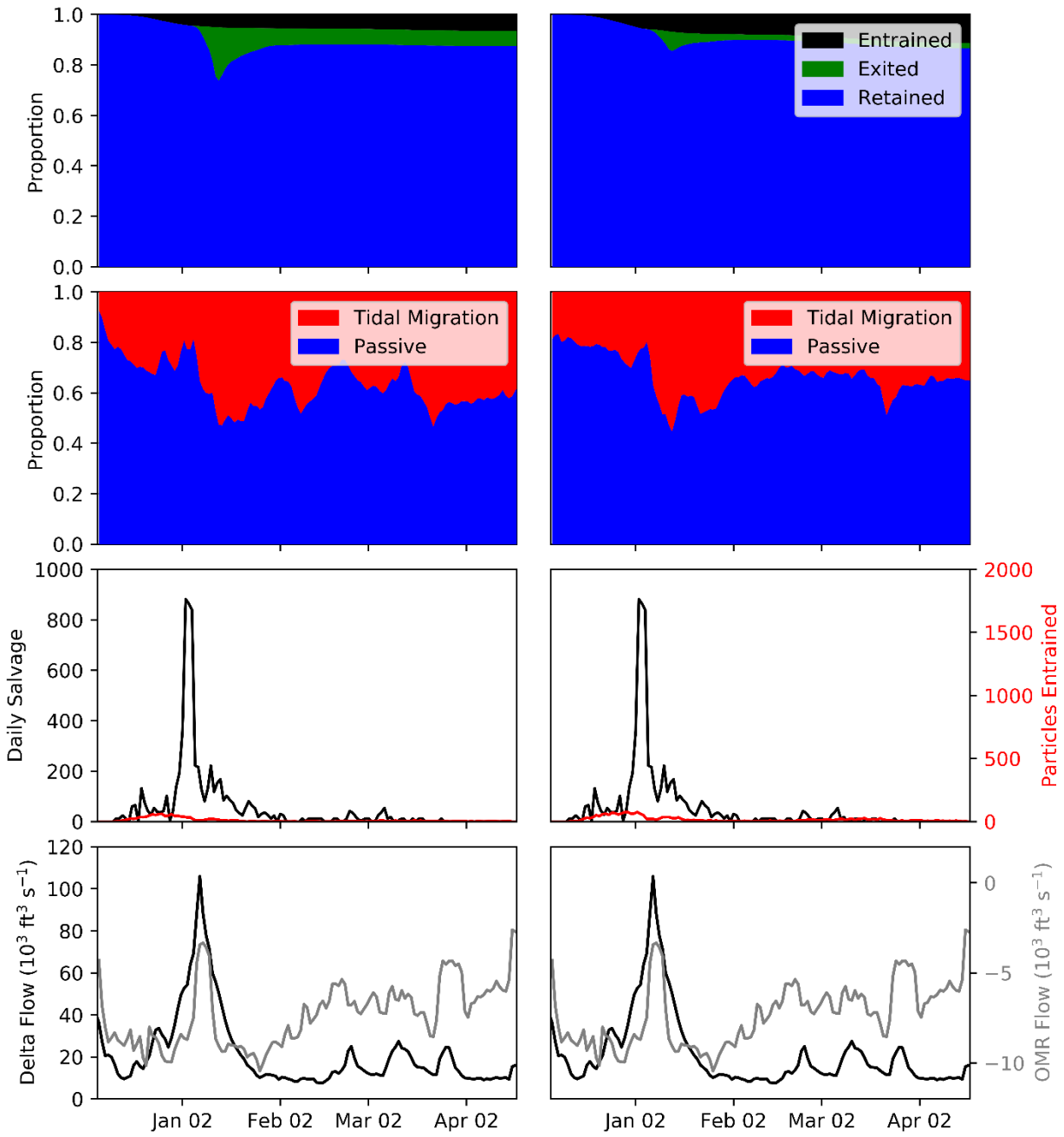

Figure 23. Results of tidal migration in brackish water behavior set (left panel) and persistent tidal migration in brackish water behavior set (right panel) for three-dimensional model, water year 2002. See caption for Figure 11.

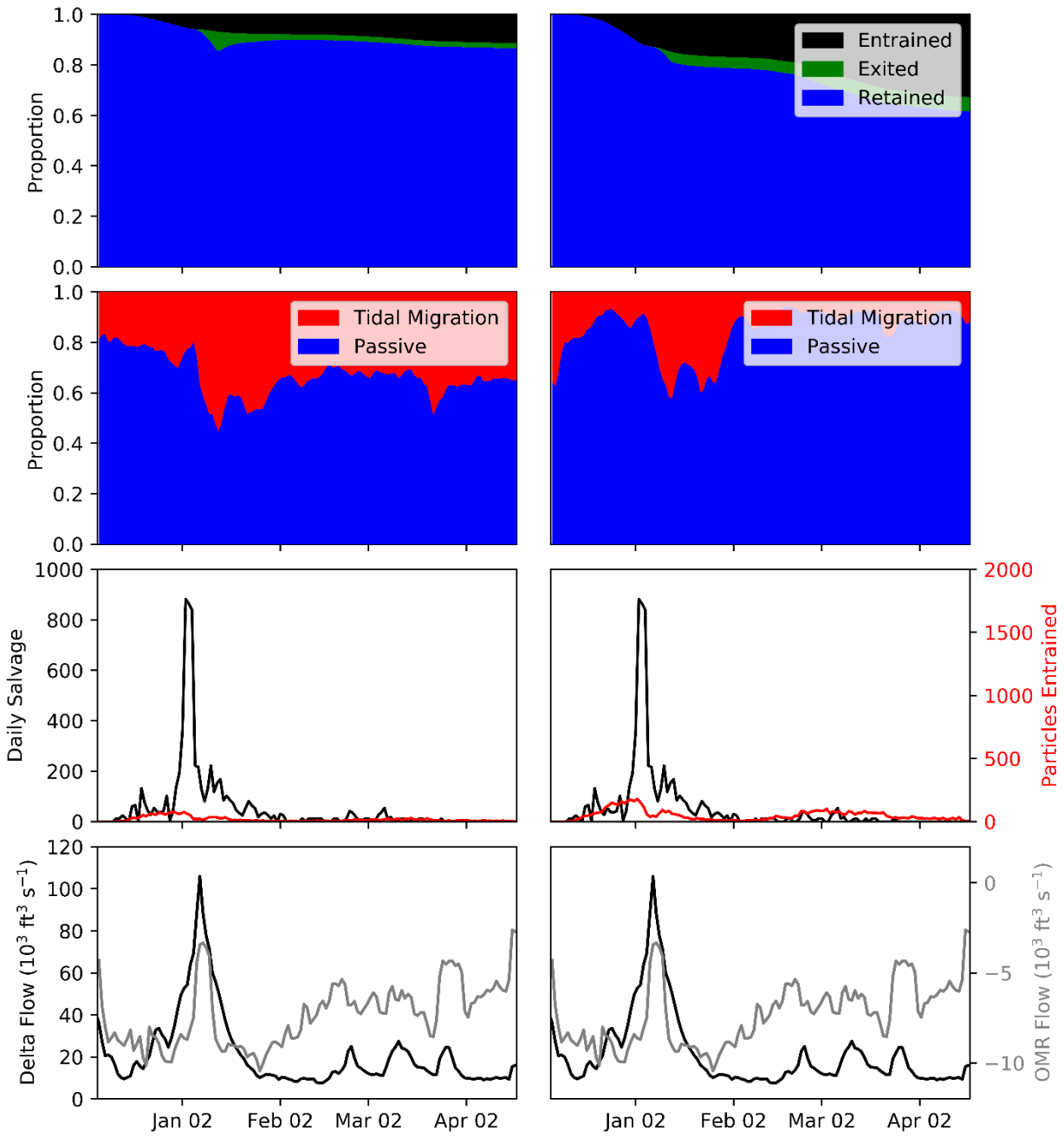

Figure 24. Results of persistent tidal migration in brackish water behavior set (left panel) and persistent tidal migration in increasing salinity behavior set (right panel) for three-dimensional model, water year 2002. See caption for Figure 11.

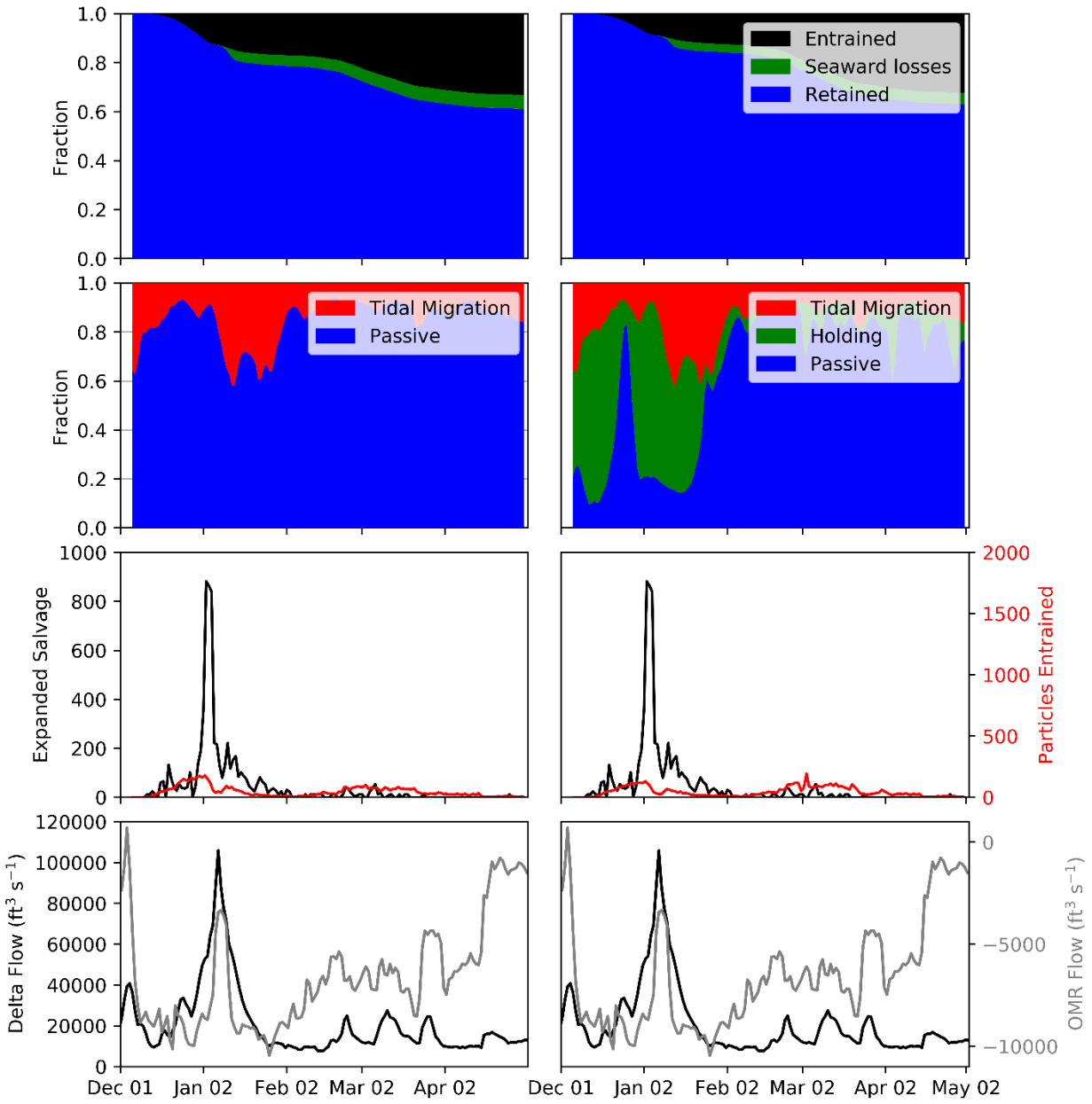

Figure 25. Results of and persistent tidal migration in increasing salinity behavior set (left panel) and persistent tidal migration in increasing salinity, otherwise move to shallow water on ebb in turbid water behavior set (right panel) for three-dimensional model, water year 2002. See caption for Figure 11.

Behavior Ranking

The consistency of predicted distribution with observed catch and salvage is represented by the negative log likelihood as described previously. For each behavior the statistical fitting estimated initial abundance, constant and uniform daily survival (representing natural mortality), and constant salvage efficiency at the SWP and CVP as free parameters. The predicted movement and proportional distribution is completely determined by the particle-tracking results. The initial abundance was

constrained to a maximum of 5 million and the daily survival was constrained to a minimum of 0.99. Salvage efficiency was not constrained.

The negative log likelihood for each behavior set for the Dec 5, 2001 release time is shown in Figure 26. All behaviors that did not use some form of tidal migration exhibited high domain losses. Tidal migration alone also performed poorly, as could be expected from the high entrainment shown in Figure 13.

The negative log likelihood for each behavior set for the Dec 5, 2001 release time for both 3D and 2D model results is shown in Figure 27. For the majority of the behaviors the negative log likelihood for the 2D model results is similar to the negative log likelihood for the 3D model results. Notable exceptions include behaviors involving freshwater seeking.

Two-dimensional model results for each behavior set were generated for water year 2004. The negative log likelihood for each behavior set for the Dec 5, 2001 release time and Dec 12, 2003 release time for 2D model results is shown in Figure 28. There are large differences in negative log likelihood for several behaviors, with generally higher (worse) negative log likelihood for water year 2004 results. This is partially due to the unusual flow pattern in 2004, with peak flow in March which caused late season salvage (Figure 6). Despite differences in the performance of several behaviors, the best performing behaviors were fairly consistent between the two water years. For example, ptmd_sal_gt_1_h8_ebb_shallow_t_gt_18_acclim was among the lowest log likelihoods in the two different water years.

Because there is some uncertainty in the timing of the spawning migration, the sensitivity of model results to particle release time was also explored. The negative log likelihood for each behavior set for the Dec 5, 2001 release time and Dec 20, 2001 release time for 3D model results is shown in Figure 29. The negative log likelihood for each behavior set for the Dec 5, 2001 release time and Dec 20, 2001 release time for 2D model results is shown in Figure 30. The Dec 20, 2001 release time generally resulting in larger negative log likelihood for most behavior sets indicating poorer comparison to observations. However, the ranking of behavior sets by negative log likelihood was similar between the two release times. Due to the larger negative log likelihood of the Dec 20, 2001 release time, indicating poorer match to observed distribution, we have focused on the Dec 5, 2001 release time results.

The overall ranking in order of increasing negative log likelihood for each behavior set is shown in Table 1. The distribution of particles at the end of the analysis period for the 3D water year 2002 hydrodynamic scenario, is shown in order of increasing negative log likelihood in Figure 31. In this ordering the top ranked behavior is shown as the top row. The two-dimensional model results for water year 2002 and 2004 are shown in Figure 32 and Figure 33. All behaviors with poor retention are ranked near the bottom. All top ranked behavior sets show good retention but several have entrainment losses higher than suggested by previous studies (e.g. Kimmerer 2008). There are several possible reasons for that discrepancy which will be explored in Korman et al. (2018). The estimated initial abundance of delta smelt is provided in Table 2. The initial abundance is constrained to 5 million. The estimated initial abundance various substantially among hydrodynamic scenarios and behavior sets and for several behavior sets reaches the maximum of 5 million delta smelt. The initial abundance and other fitting parameters will be explored and discussed in more detail in Korman et al. (2018). It should be noted that the proportion of particles in each region is determined entirely by the particle-tracking for each behavior set and therefore the predicted distribution is the focus of this report. The coefficient of determination in predicting regional abundance estimate from expansion of Spring Kodiak Trawl catch is

provided for each behavior and hydrodynamic scenario in Table 3. The particle-tracking for each behavior set also determines the timing of predicted entrainment though the survival parameter can alter the magnitude of late season predicted entrainment relative to earlier season entrainment to a limited extent.

Several behaviors are ranked high for all three hydrodynamic scenarios. Specifically, the behavior sets ptmd_sal_gt_1_h8_ebb_shallow_t_gt_18_acclim, tmd_sal_gt_1_ebb_shallow_t_gt_18, and tmd_sal_gt_1_ptmd_prtmd_sd_pt_1_switch are each top ranked in one hydrodynamic scenario and within the top 6 ranked behavior sets for all 3 hydrodynamic scenarios. Therefore, these behaviors have all been selected for further analysis which will including fitting an initial distribution and further exploration of salvage efficiency. Because all three of those top ranked behavior had relatively high entrainment, two moderate entrainment scenarios, ptmd_si_pt_5_h8_t_gt_18_acclim and ptmd_sal_gt_1_si_pt_5, were also chosen more subjectively based on middle to high ranking, simplicity and moderate entrainment. The simplest scenarios including passive, turbidity seeking and tidal migration were also included for further analysis as those behavior types have been discussed in the literature. Lastly, since the top ranked behaviors all involve some form of salinity triggered tidal migration, both ptmd_sal_gt_1 and ptmd_si_pt_5 were also selected.

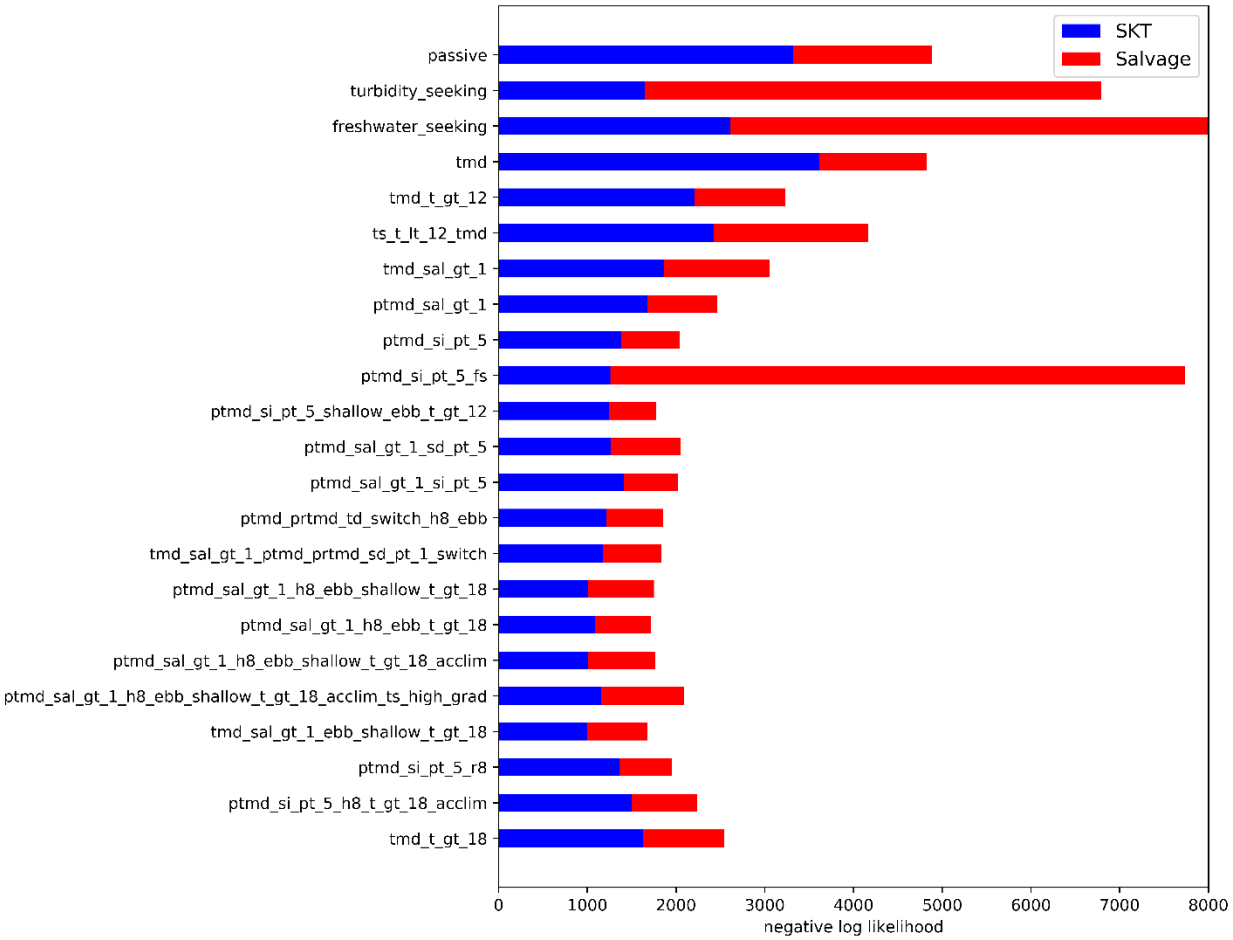

Figure 26. Three-dimensional model results for the Dec 5, 2001 release time. Blue bars indicate the portion of negative log likelihood associated with the comparison of predicted regional abundance with Spring Kodiak Trawl catch while the red bars indicate the portion of negative log likelihood associated the comparison of predicted entrainment with entrained based on observed daily salvage and salvage efficiency parameters. Results plotted as negative log likelihood so that shorter bars indicate more consistency between model results and observations. A description of the behavior set associated with each bar is given in Appendix A.

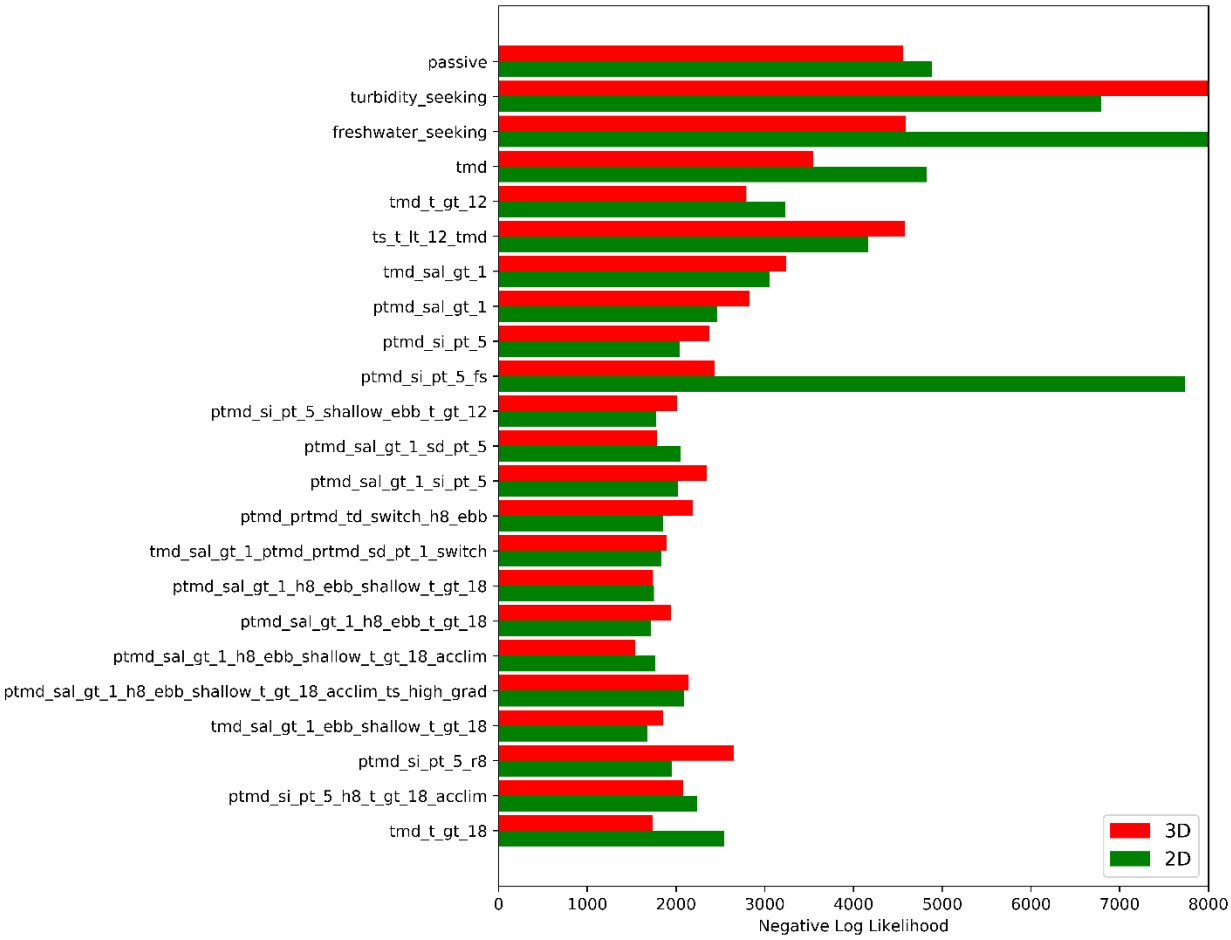

Figure 27. Negative log likelihood associated with three-dimensional and two-dimensional model results for Dec 5, 2001 release time. Each bar shows negative the log likelihood based on comparison with Spring Kodiak Trawl catch and observed daily salvage. Shorter bars indicate better results. A description of the behavior set associated with each bar is given in Appendix A.

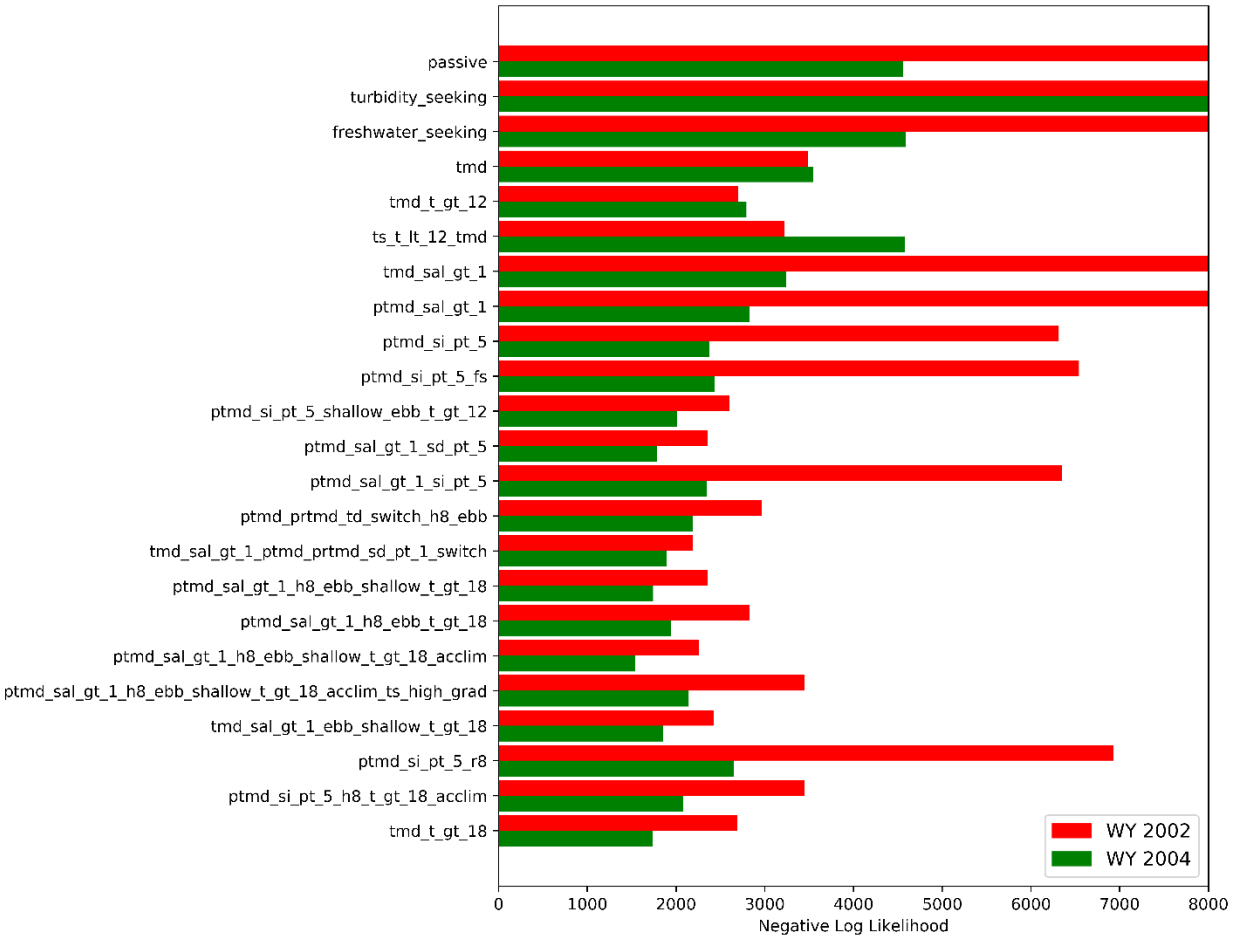

Figure 28. Negative log likelihood associated with two-dimensional model results for Dec 5, 2001 release time and Dec 12, 2003 release time. See caption for Figure 27.

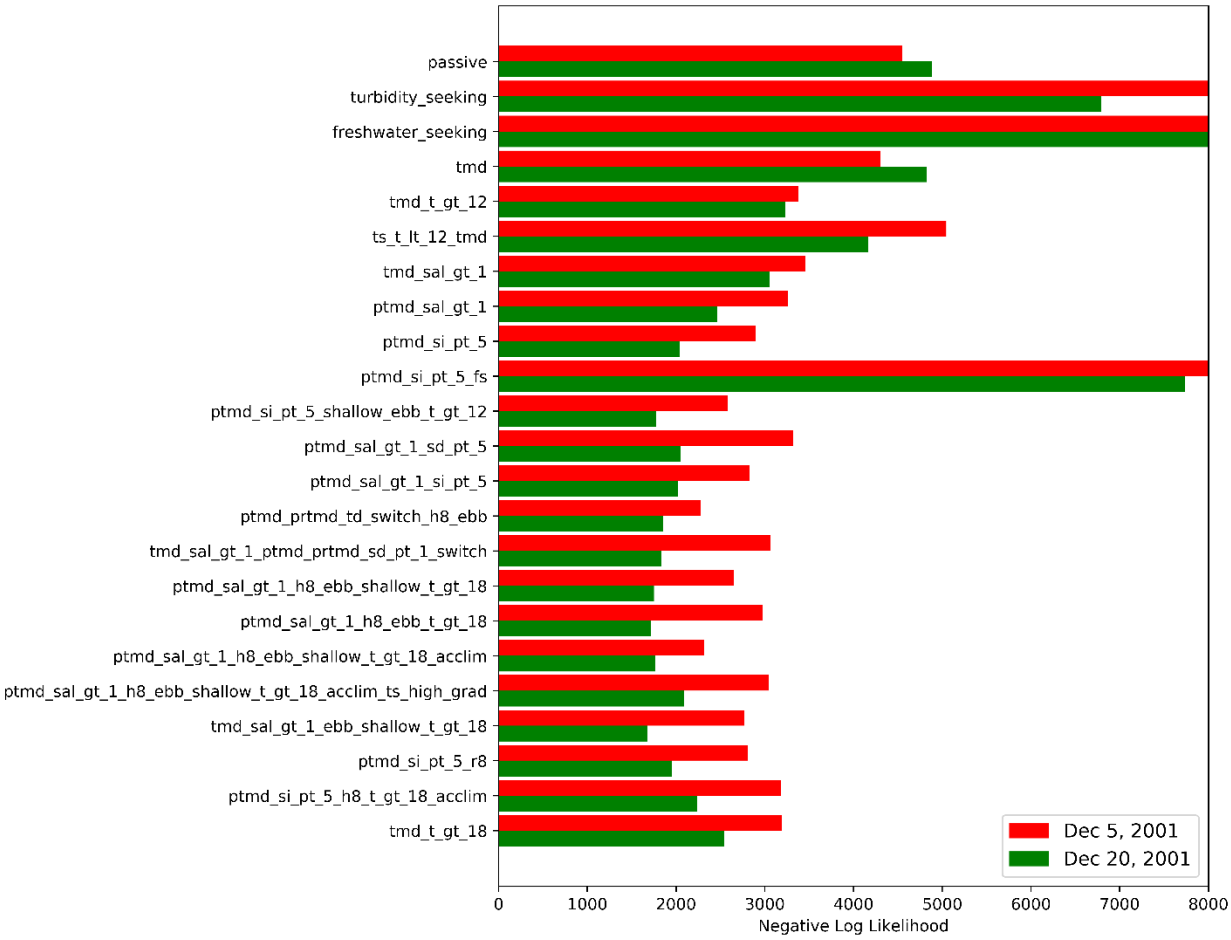

Figure 29. Negative log likelihood associated with three-dimensional model results for Dec 5, 2001 release time and Dec 20, 2001 release time. See caption for Figure 27.

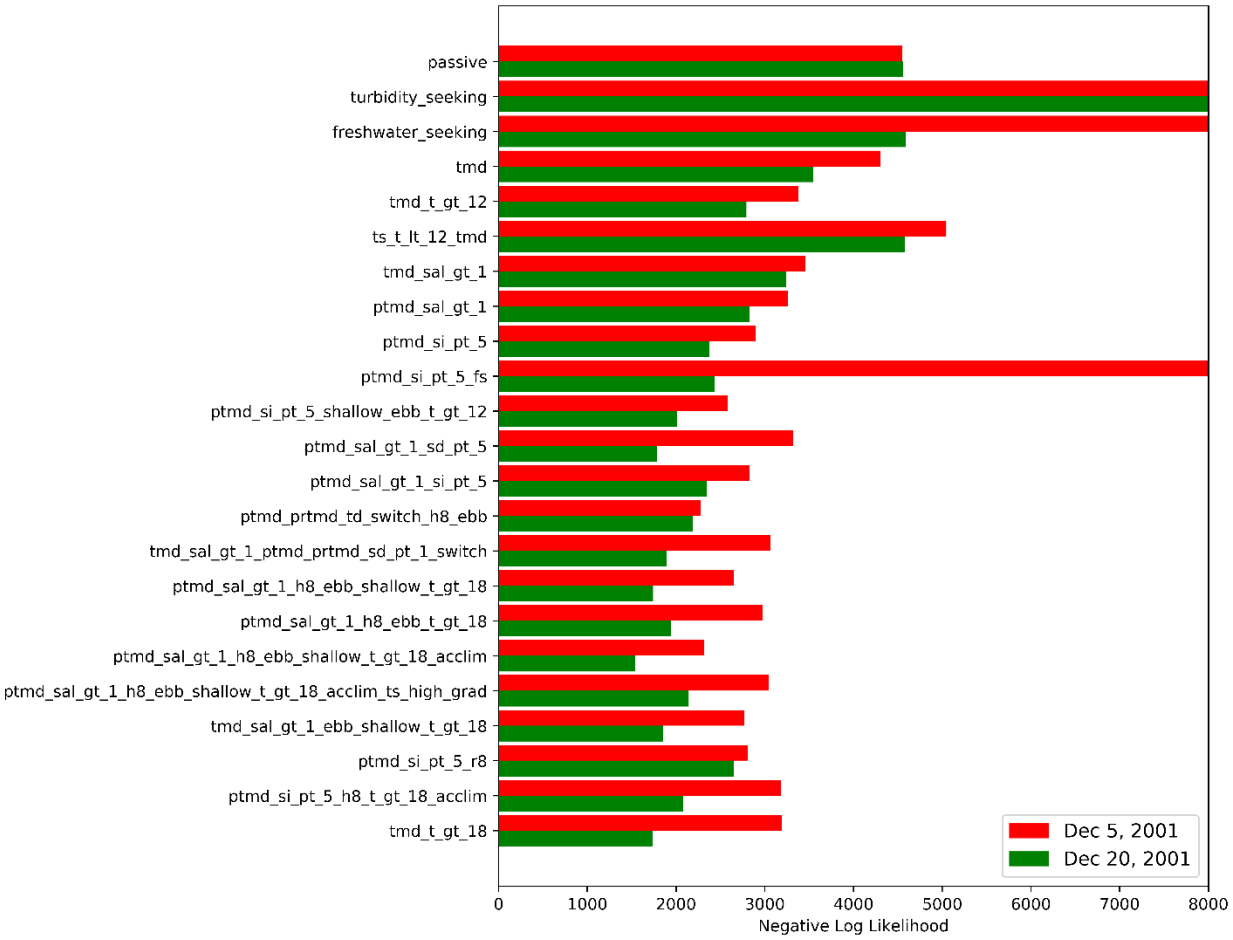

Figure 30. Negative log likelihood associated with two-dimensional model results for Dec 5, 2001 release time and Dec 20, 2001 release time. See caption for Figure 27.

Table 1. Ranking of behavior sets by increasing negative log likelihood for individual hydrodynamic scenarios.

Behavior	**Rank**			
	3D 2002	**2D 2002**	**2D 2004**	**Average**
ptmd_sal_gt_1_h8_ebb_shallow_t_gt_18_acclim	4	1	2	2.33
ptmd_sal_gt_1_h8_ebb_shallow_t_gt_18	3	3	4	3.33
tmd_sal_gt_1_ebb_shallow_t_gt_18	1	5	5	3.67
tmd_sal_gt_1_ptmd_prtmd_sd_pt_1_switch	6	6	1	4.33
ptmd_sal_gt_1_sd_pt_5	11	4	3	6.00
ptmd_sal_gt_1_h8_ebb_t_gt_18	2	7	9	6.00
ptmd_si_pt_5_shallow_ebb_t_gt_12	5	8	6	6.33
tmd_t_gt_18	15	2	7	8.00
ptmd_prtmd_td_switch_h8_ebb	7	11	10	9.33
ptmd_sal_gt_1_h8_ebb_shallow_t_gt_18_acclim_ts_high_grad	12	10	12	11.33
ptmd_si_pt_5_h8_t_gt_18_acclim	13	9	13	11.67
ptmd_sal_gt_1_si_pt_5	9	12	16	12.33
ptmd_si_pt_5	10	13	15	12.67
tmd_t_gt_12	17	16	8	13.67
ptmd_si_pt_5_r8	8	15	18	13.67
ptmd_sal_gt_1	14	17	19	16.67
ts_t_lt_12_tmd	18	21	11	16.67
Tmd	19	19	14	17.33
ptmd_si_pt_5_fs	22	14	17	17.67
tmd_sal_gt_1	16	18	21	18.33
Passive	20	20	20	20.00
turbidity_seeking	21	23	23	22.33
freshwater_seeking	23	22	22	22.33

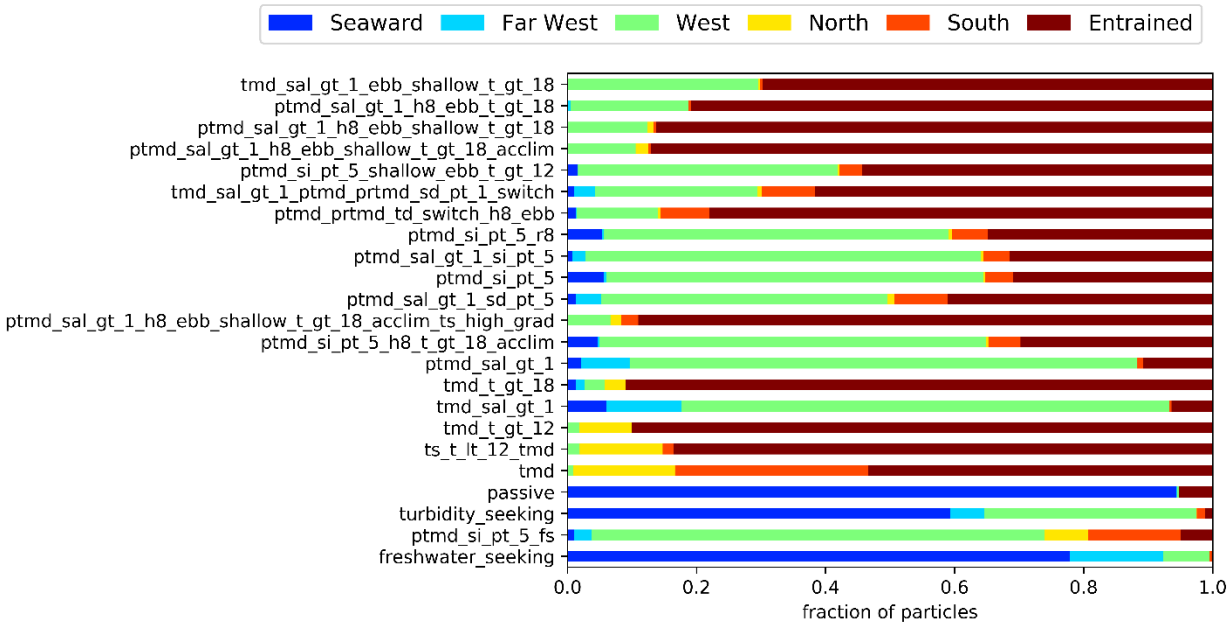

Figure 31. Particle distribution at the end of the simulation period in order of increasing negative log likelihood for the three-dimensional model results for water year 2002. In this ordering the best performing behavior set is the top row.

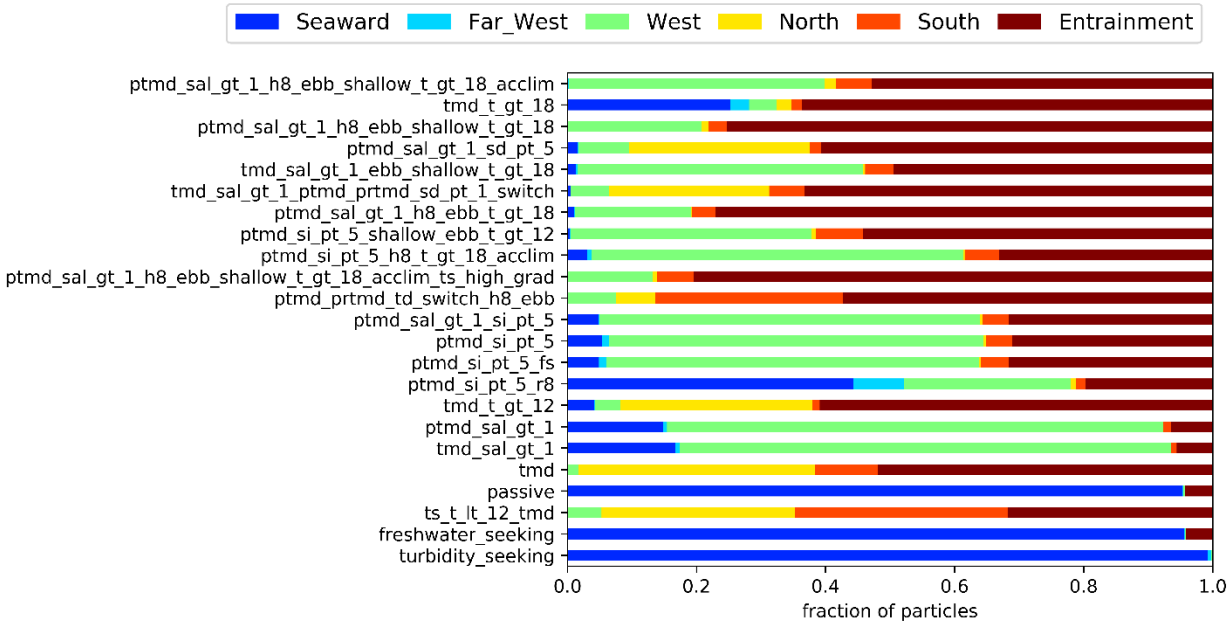

Figure 32. Particle distribution at the end of the simulation period in order of increasing negative log likelihood for the two-dimensional model results for water year 2002. In this ordering the best performing behavior set is the top row.

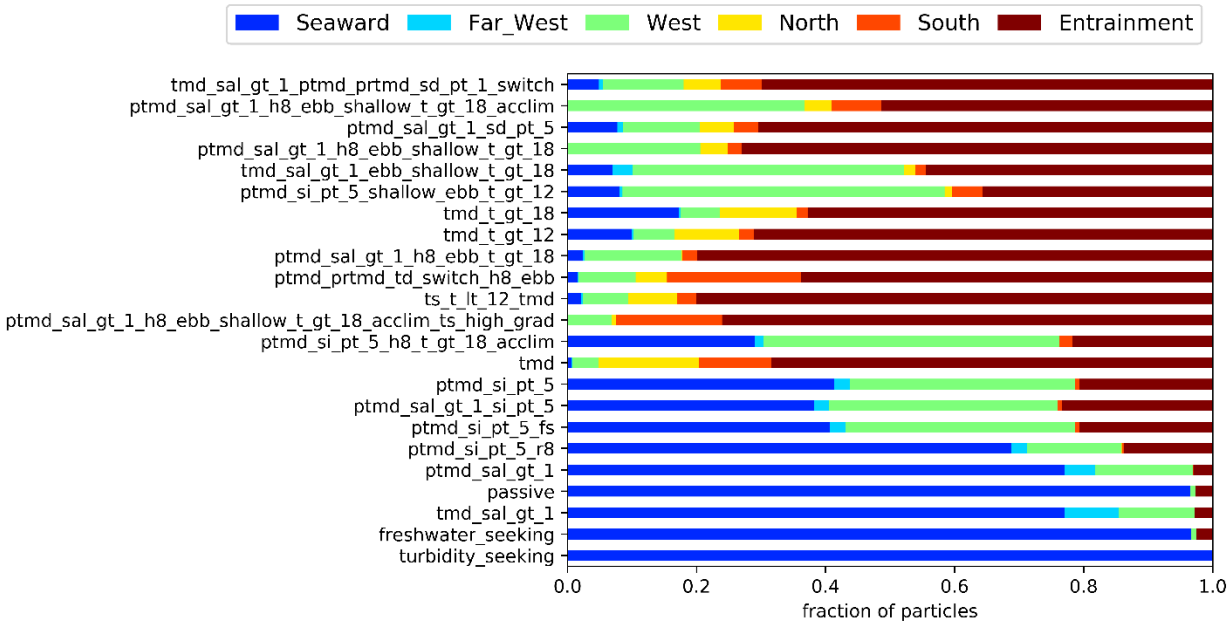

Figure 33. Particle distribution at the end of the simulation period in order of increasing negative log likelihood for the two-dimensional model results for water year 2004. In this ordering the best performing behavior set is the top row.

Table 2. Initial abundance of delta smelt estimated by statistical fitting approach for each hydrodynamic scenario and behavior set.

Behavior	Initial Abundance			
	3D 2002	2D 2002	2D 2004	Average
ptmd_sal_gt_1_h8_ebb_shallow_t_gt_18_acclim	4108430	2201310	1265230	2524990
ptmd_sal_gt_1_h8_ebb_shallow_t_gt_18	3835260	2459460	1630940	2641887
tmd_sal_gt_1_ebb_shallow_t_gt_18	2016970	2998520	1105280	2040257
tmd_sal_gt_1_ptmd_prtmd_sd_pt_1_switch	3372280	3156160	1752580	2760340
ptmd_sal_gt_1_sd_pt_5	2728070	3908340	1781980	2806130
ptmd_sal_gt_1_h8_ebb_t_gt_18	3275870	2987820	2126940	2796877
ptmd_si_pt_5_shallow_ebb_t_gt_12	3212940	3605730	1427520	2748730
tmd_t_gt_18	5000000	4669210	2733340	4134183
ptmd_prtmd_td_switch_h8_ebb	2785920	2349390	1854510	2329940
ptmd_sal_gt_1_h8_ebb_shallow_t_gt_18_acclim_ts_high_grad	5000000	2422490	2707370	3376620
ptmd_si_pt_5_h8_t_gt_18_acclim	2677140	2384630	1230730	2097500
ptmd_sal_gt_1_si_pt_5	2306470	2462100	1243280	2003950
ptmd_si_pt_5	2611660	2511790	1277700	2133717
tmd_t_gt_12	5000000	2940870	2776600	3572490
ptmd_si_pt_5_r8	2649580	3954610	2475620	3026603
ptmd_sal_gt_1	2240750	3444070	1918560	2534460
ts_t_lt_12_tmd	5000000	2474470	2766020	3413497
Tmd	2258580	2226860	2065920	2183787
ptmd_si_pt_5_fs	1005830	2590630	1221750	1606070
tmd_sal_gt_1	2661320	3545950	1927260	2711510
Passive	5000000	5000000	5000000	5000000
turbidity_seeking	2118090	5000000	2463190	3193760
freshwater_seeking	1839780	5000000	5000000	3946593

Table 3. Coefficient of determination in predicting regional abundance estimated from Spring Kodiak Trawl expansion for each behavior and hydrodynamic scenario.

	Coefficient of Determination		
Behavior	**3D 2002**	**2D 2002**	**2D 2004**
passive	0.031909	0.024486	0.237229
turbidity_seeking	0.57465	0.002381	0.005482
freshwater_seeking	0.123905	0.01833	0.221913
Tmd	0.016814	3.92E-05	5.09E-07
tmd_t_gt_12	0.001676	0.002002	0.018665
ts_t_lt_12_tmd	0.000721	0.001335	0.002388
tmd_sal_gt_1	0.013339	0.00023	0.003026
ptmd_sal_gt_1	0.095532	0.000667	0.002901
ptmd_si_pt_5	0.129063	0.064214	0.16394
ptmd_si_pt_5_fs	0.293752	0.064442	0.17096
ptmd_si_pt_5_shallow_ebb_t_gt_12	0.266572	0.041185	0.111315
ptmd_sal_gt_1_sd_pt_5	0.16249	0.061786	0.094033
ptmd_sal_gt_1_si_pt_5	0.212715	0.069109	0.198578
ptmd_prtmd_td_switch_h8_ebb	0.416543	0.032855	0.002429
tmd_sal_gt_1_ptmd_prtmd_sd_pt_1_switch	0.274307	0.066921	0.20091
ptmd_sal_gt_1_h8_ebb_shallow_t_gt_18	0.478761	0.425944	0.297024
ptmd_sal_gt_1_h8_ebb_t_gt_18	0.487087	0.240771	0.396036
ptmd_sal_gt_1_h8_ebb_shallow_t_gt_18_acclim	0.457475	0.504375	0.333959
ptmd_sal_gt_1_h8_ebb_shallow_t_gt_18_acclim_ts_high_grad	0.169067	0.178971	0.003889
tmd_sal_gt_1_ebb_shallow_t_gt_18	0.639325	0.249303	0.45373
ptmd_si_pt_5_r8	0.153901	0.004818	0.025226
ptmd_si_pt_5_h8_t_gt_18_acclim	0.079391	0.143412	0.098852
tmd_t_gt_18	0.021786	0.09594	0.015121

Discussion

We compared the relative performance of several alternative sets of delta smelt swimming behavior rules. A tidal migration behavior has been discussed in past publications (e.g. Sommer et al. 2011) as a likely spawning migration behavior leading to rapid landward movement of delta smelt. The simulations here are consistent with those expectations in that it does lead to rapid landward migration. However, a less well-established aspect of the tidal migration is the cue (or cues) to trigger initiation or cessation of tidal migration. If the simulated tidal migration behavior continues without regard to turbidity or other environmental cues it leads to high entrainment losses.

Bennett and Burau (2014) also report evidence of tidal migration behavior but further hypothesize that this tidal migration may be driven by the combination of smelt seeking higher turbidity and the tidal phasing of turbidity gradients. A simple behavior driven by turbidity cues is swimming in the direction of

higher turbidity. This representation of behavior leads to poor predicted retention. Salinity has also been used as an environmental cue in delta smelt simulations (Rose et al. 2013). A simple salinity driven swimming response is swimming in the horizontal direction of decreasing salinity. Similar to the turbidity seeking behavior and passive behavior, this lead to poor retention in the estuary. However, a salinity triggered tidal migration behavior led to good retention.

Of the scenarios explored, the behavior rules which do not allow behavior to vary in time lead to unrealistic predictions of delta smelt distribution and fate. Tidal migration is too extreme in terms of shifting particles in the landward direction and the other simple behaviors retain particles poorly. The observed distributions of delta smelt suggest that a more realistic behavior should have an outcome intermediate to these extremes. As suggested by Bennett and Burau (2014) and other authors, it is likely that actual delta smelt swimming behavior can vary through time. For example, it may involve tidal migration but only during certain environmental conditions and may involve additional elements such as avoidance of deep channel (Bennett and Burau 2014), holding behavior in favorable habitat or prior to spawning (Sommer et al. 2011), or day-night variability (Bennet 2005). Triggers may also be more complex, for example relating to the perceived change in environmental properties that a particle experiences moving through the estuary (Goodwin et al. 2014). Several sets of behavior rules explored represent more complex behaviors which involve tidal migration under selective conditions such as high turbidity or a perceived increase in salinity.

The predicted particle fate for the simpler behaviors are broadly consistent with respect to particle release time and modeling tools applied. For example, turbidity seeking leads to poor retention for both the 2D and 3D tools. The predicted distributions associated with behaviors triggered by environmental stimuli, such as tidal migration when turbidity is perceived by a particle to be increasing, lead to larger differences in predicted fate between the 2D and 3D model. This is likely in part due to the substantial differences in predicted turbidity fields between the 2D and 3D models.

Avoidance of high salinity is one behavior that has somewhat consistent and predictable outcomes among scenarios. This behavior leads to good retention of particles and low entrainment. To a large extent persistent tidal migration when salinity is perceived to be increasing mimics this behavior because tidal migration is generally triggered when particles enter higher salinity, leading to retention in low salinity regions.

While there was variation in negative log likelihood between 2D and 3D and with particle release time, some were more robust than others. There was particular support for the conclusion that high or increasing salinity may trigger tidal migration. That response was also represented in previous modeling studies (RMA 2009). There was less success of behaviors with only turbidity-based triggers in reproducing observed distributions but that may be partially due to the higher uncertainty of turbidity predictions.

Two closely related questions motiving this work are 1) which environmental conditions trigger initiation of the spawning migration of delta smelt? and 2) which environmental conditions lead to adults entering the south Delta. After consultation with the CAMT DSST, we chose to start the simulations at a time thought to correspond roughly to the beginning of the spawning migration based on the arrival at Rio Vista of turbid water associated with a “first flush” event of each year. For each behavior evaluated, this allowed the assumption of a single set of behavior rules during the whole simulation period as opposed to a discrete switch from behavior rules prior to the spawning migration to spawning migration behavior

rules. Releasing particles at a time significantly prior to the spawning migration would introduce ambiguity, in attributing differences between observed and predicted distributions to: 1) uncertainties in representation of pre-spawning migration; 2) uncertainties in the trigger for initiation of spawning migration; or 3) uncertainties in representation of spawning migration behavior. However, behaviors that are relatively high ranked in both the Dec 5, 2001 release results and the Dec 20, 2001 release results generally involve salinity triggered tidal migration, suggesting that is a likely behavior both prior to and during the spawning migration. Several of the consistently high ranked behaviors also involve variations of holding in turbid water which generally lead to less seaward movement. Therefore, there is some support for a turbidity trigger resulting in a landward shift in distribution associated with the spawning migration. Table 1 indicates that the turbidity level which triggered holding behaviors was 18 NTU for the three highest ranked behaviors.

While some behavior sets yielded predicted distributions much more consistent with observed delta smelt distributions than other behavior sets, there were some biases common among most of the highest ranked behaviors. First, the predicted proportion of particles entrained was higher than estimated in Kimmerer et al. (2008) and may be unrealistic. Further support of overestimate of entrainment can be seen in the figures in Appendix B which indicate that best performing behaviors typically overestimate south Delta abundance. Two non-exclusive explanations seem most likely. One is that the behavior sets are missing a component of the actual delta smelt behavior that results in avoidance of the south Delta. The other is that the overestimate of entrainment and south Delta abundance may both be related in part to the use of spatially uniform natural mortality in this study. If south Delta natural mortality was higher than natural mortality in other regions, the use of uniform natural mortality would lead to overestimate both of south Delta abundance and entrainment. Variation in catchability of delta smelt with respect to turbidity in the Spring Kodiak Trawl surveys may also contribute to the discrepancy between predicted and observed south Delta abundance. While that one region contributes little to the overall log likelihood estimates it is particularly important for predicted entrainment.

All the behaviors explored so far share several simplifying assumptions. One is lack of stochasticity in swimming response. All responses occur at threshold levels each particle responds at the same threshold as other particles. Similarly, swimming speed is uniform among particles and direction is also fully deterministic (e.g. in the direction of shallower water) for most behaviors. Variability in behavior with life stage or and diel (day-night) variability are not considered. However, each behavior involves free parameters, such as the turbidity or salinity required to trigger tidal migration. In additional simulations not reported here we explored sensitivity to most of these parameters. However, due to the substantial computational expense of each behavior scenario simulated we have not done an automated fitting of behavior parameters so may not have found near optimal parameter values for the candidate behaviors.

While it is certain that none of the behaviors is a full description of actual delta smelt swimming behavior, several other uncertainties not related to the sets of behavior rules may limit accuracy of these distribution and entrainment predictions. A primary uncertainty is the accuracy and resolution required of the hydrodynamic model predictions. A limitation in both models is representation of nearshore velocity. Actual delta smelt are likely to be able to find small scale quiescent regions in shallow water, or small-scale eddies that are not resolved by the hydrodynamic models. In addition, the accuracy of turbidity predictions may not be adequate for the purposes of evaluating turbidity driven

behaviors. Comparisons to Secchi depth data suggested that turbidity in the central and south Delta is underestimated by both the 2D and 3D modeling tools in water year 2002 (Pete Smith, personal communication). This calls into question whether behaviors with turbidity cues have realistic responses. Behaviors that depend on turbidity gradients, such as turbidity seeking, or are triggered by perceived change in turbidity may be sensitive to the degree of patchiness of predicted turbidity fields. The turbidity fields predicted by RMA2 tools tend to be smoother than those predicted by UnTRIM and SediMorph. The ability to predict small scale turbidity gradients has not been explicitly evaluated so it is not clear if either set of tools is adequately predicting turbidity gradients for purposes of delta smelt behavior modeling. Salinity fields are more similar between the two models and calibrated at far more observation stations so is believed to be predicted more reliably.

The differences between observed catch and predicted distribution may also involve factors in addition to inaccuracy in the turbidity field or representation of swimming behavior of delta smelt. Uncertainty associated with initial distribution and release time of particles may be substantial. Latour (2016) reported significant variation in catch per unit effort (CPUE) with Secchi depth. Therefore, the actual distribution of delta smelt may vary from the distribution implied by CPUE effort in the FMWT surveys due to spatial variability in turbidity. The potential sensitivity to timing of the release was explored by simulating both a December 5, 2001 and December 20, 2001 release time and found to be significant though most of the best performing models for the earlier release also performed relatively well for the later release. Additional factors that will be explored to some extent in Korman et al. (2018) include temporal variability in salvage efficiency driven by mortality or other factors, temporal variability in natural mortality, and initial distribution of delta smelt.

Conclusions

The predicted distribution and fate of particles varied greatly with specified swimming behavior. Some but not all behaviors evaluated were adequate to offset seaward transport by net flows experienced by passive particles. Among the behaviors that resulted in retention of particles, predicted entrainment ranged from near zero to the dominant fate of particles.

The simplest representations of delta smelt swimming behavior did not produce realistic distributions. The observed distribution based on estimates of abundance in Spring Kodiak Trawl surveys appears to find a fine balance between enough tidal migration to be retained in the northern estuary and not so much tidal migration to result in excessive entrainment in water export facilities. The modeling results here suggest that somewhat realistic outcomes can be achieved by some form of selective tidal migration. It particularly shows support for tidal migration triggered by high salinity or perceived increases in salinity. There is much less certainty about what additional environmental stimuli may trigger tidal migration behavior and the cessation of tidal migration behavior or which additional behaviors (e.g. holding) may be exhibited by delta smelt.

The sets of behavior rules selected here will be explored further in additional simulations which do not assume a given initial distribution (Korman 2018). These simulations will allow fitting of initial regional abundance and will incorporate Fall Midwater Trawl Survey observations in addition to Spring Kodiak Trawl observations to fit initial regional abundance and additional parameters. Korman et al. (2018) will also discuss additional factors that may contribute to observed catch and salvage patterns, including spatial variability in natural mortality, and variation in salvage efficiency with turbidity.

References

Anchor QEA, 2017. Collaborative Adaptive Management Team Investigations on Understanding Factors that Affect Entrainment of Delta Smelt, Hydrodynamic and Sediment Transport Modeling Study, December 2017.

Ahrestani FS, Hebblewhite M, Post E. 2013. The importance of observation versus process error in analyses of global ungulate populations. Scientific Reports 3:3125. DOI: 10.1038/srep03125.

BAW, 2005. Mathematical Module SediMorph, Validation Document, Version 1.1, The Federal Waterways Engineering and Research Institute.

Bennett, WA. 2005. Critical assessment of the delta smelt population in the San Francisco Estuary, California. San Francisco Estuary and Watershed Science. Available from htt://www.escscholarship.org/uc/item/0725n5vk

Bennett WA, Burau JR. 2015. Riders on the storm: Selective tidal movements facilitate the spawning migration of threatened delta smelt in the San Francisco Estuary. Estuaries and Coasts 38: 826–835.

Bever AJ and MacWilliams ML. 2013. Simulating sediment transport processes in San Pablo Bay using coupled hydrodynamic, wave, and sediment transport models. Marine Geology. 345, 235-253. http://dx.doi.org/10.1016/j.margeo.2013.06.012

Brown LR, Kimmerer WJ, and Brown R. 2009. Managing water to protect fish: A review of California's environmental water account, 2001–2005. Environmental Management 43:357–368.

Casulli V, Walters RA. 2000. An unstructured, three-dimensional model based on the shallow water equations, International Journal for Numerical Methods in Fluids, 32: 331 - 348.

[CDWR] California Department of Water Resources, 2016a. Chronological Reconstructed Sacramento and San Joaquin Valley Water Year Hydrological Classification Indices. ⟨http://cdec.water.ca.gov/cgi-progs/iodir/wsihist⟩. (Accessed 5 July 2016).

[CDWR] California Department of Water Resources, 2016b. Dayflow, An Estimate of Daily Average Delta Outflow. ⟨http://www.water.ca.gov/dayflow⟩. (Accessed 5 July 2016).

Feyrer F, Nobriga ML, Sommer TR. 2007. Multidecadal trends for three declining fish species: habitat patterns and mechanisms in the San Francisco Estuary, California, USA. Can J Fish Aquat Sci 64:723–734. doi: http://dx.doi.org/10.1139/f07-048

Fournier DA, Skaug HJ, Ancheta J, Ianelli J, Magnusson A, Maunder MN, Nielsen A, Sibert J. 2011. AD Model Builder: using automatic differentiation for statistical inference of highly parameterized complex nonlinear models. Optimization Methods & Software. Available from http://admb-project.org/ [accessed 17 February 2012].

Goodwin RA, Politano M, Garvin,JW, Nestler JM, Hay D, Anderson JJ, Weber LJ, Dimperio E, Smith DL, Timko MA. 2014. Fish navigation of large dams emerges from their modulation of flow field experience. Proceedings of the National Academy of Sciences, 111, 5277-5282.

Grimaldo LF, Sommer T, Van Ark N, Holland E, Jones G, Herbold B, Smith P, Moyle P. 2009. Factors affecting fish entrainment into massive water diversions in a freshwater tidal estuary: Can fish losses be managed?" North American Journal of Fisheries Management 29:1253–1270.

Hammock BG, Hobbs JA, Slater SB, Acuña S, Teh SJ. 2015. Contaminant and food limitation stress in an endangered estuarine fish. Sci Total Environ 532:316–326. doi: http://dx.doi.org/10.1016/j.scitotenv.2015.06.018

Ketefian GS, Gross ES, Stelling GS. 2016. Accurate and consistent particle tracking on unstructured grids, International Journal for Numerical Methods in Fluids, 80(11): 648–665, doi:10.1002/fld.4168.

Kimmerer WJ. 2008. Losses of Sacramento River Chinook Salmon and Delta Smelt to Entrainment in Water Diversions in the Sacramento-San Joaquin Delta. *San Francisco Estuary and Watershed Science*, 6(2), Retrieved from: http://escholarship.org/uc/item/7v92h6fs

King IP. 1986. "Finite Element Model for Two-Dimensional Depth Averaged Flow, RMA2V, Version 3.3", Resource Management Associates.

Korman J, Gross ES, Smith PE, Saenz B, Grimaldo LF. 2018. Statistical Evaluation of Particle-Tracking Models Predicting Proportional Entrainment Loss for Adult Delta Smelt in the Sacramento-San Joaquin Delta. Report to the CAMT DSST.

Lai YG, Goodwin A, Smith DL, Reeves RL. 2017. Complex Unsteady Flow Patterns at a River Junction and Their Relation with Fish Movement Behavior. World Environmental and Water Resources Congress 2017: 8-14.

Moyle PB, Brown LR, Durand JR, and Hobbs JA. 2016. Delta smelt: Life history and decline of a once-abundant species in the San Francisco Estuary. San Francisco Estuary and Watershed Science 14: 1–30.

Murphy DD, Hamilton, SA. 2013. Eastward Migration or Marshward Dispersal: Exercising Survey Data to Elicit an Understanding of Seasonal Movement of Delta Smelt. San Francisco Estuary and Watershed Science, 11(3). Jmie_sfews_15805.

Newman K, Polansky L, and Mitchell L. 2015. Adult Delta Smelt entrainment estimation and monitoring plan (draft May 24, 2015).

Polansky L, Newman KB, Nobriga ML, Mitchell L. 2017. Spatiotemporal Models of an Estuarine Fish Species to Identify Patterns and Factors Impacting Their Distribution and Abundance. Estuaries and Coasts. DOI 10.1007/s12237-017-0277-3.

Resource Management Associates. 2009. Particle Tracking and Analysis of Adult and Larval/Juvenile Delta Smelt for 2-Gates Demonstration Project, Draft report prepared for Metropolitan Water District of Southern California, 2009, http://www.baydeltalive.com/-/catalog/download.php?f=/assets/05058ccde7595f531c3f6b5eda7faa2f/application/pdf/Appendix_B._Particle_Tracking_and_Analysis_of_Adult_and_Larval_Juvenile_Delta_Smelt.pdf

Resource Management Associates. 2017. Calibration of the Hydrodynamic, Salinity and Turbidity Models for the Adult Delta Smelt Behavior Study. Report for the Collaborative Adaptive Management Team.

Rose KA, Kimmerer WJ, Edwards KP, Bennett WA. 2013. Individual-based modeling of delta smelt population dynamics in the upper San Francisco Estuary: I. Model description and baseline results. Transactions of the American Fisheries Society 142: 1238–1259.

Schoellhamer DH. 2011. Sudden clearing of estuarine waters upon crossing the threshold from transport to supply regulation of sediment transport as an erodible sediment pool is depleted: San Francisco Bay, 1999. Est Coasts 34(5):885-899

Sommer T, Mejia F, Nobriga M, Feyrer F, Grimaldo L. 2011. The Spawning Migration of Delta Smelt in the Upper San Francisco Estuary. San Francisco Estuary and Watershed Science 9(2), 16 pages.

Sommer, T. and F. Mejia, 2013, A Place to Call Home: A Synthesis of Delta Smelt Habitat in the Upper San Francisco Estuary, San Francisco Estuary and Watershed Science 11(2).

SWAN Team. 2009. SWAN Scientific and Technical Documentation 40.72. Delft University of Technology.

Swanson C, Young PS, Cech JJ Jr (1998) Swimming performance of delta smelt: maximum performance, and behavioral and kinematic limitations on swimming at submaximal velocities. J Exp Biol 201:333–345